Non-monsoon precipitation response over the western Himalayas to climate change

R. Krishnan

Centre for Climate Change Research (CCCR)
Indian Institute of Tropical Meteorology, Pune
Ministry of Earth Sciences, Govt of India

Collaborators: T.P. Sabin, Madhura H.K., Vellore R., Mujumdar M., Sanjay J., Nayak S., and Rajeevan M.

TROPMET 2018: National Symposium on
Understanding Weather and Climate Variability: Research for Society
24-27 October, 2018
Banaras Hindu University, Varanasi, Uttar Pradesh, India

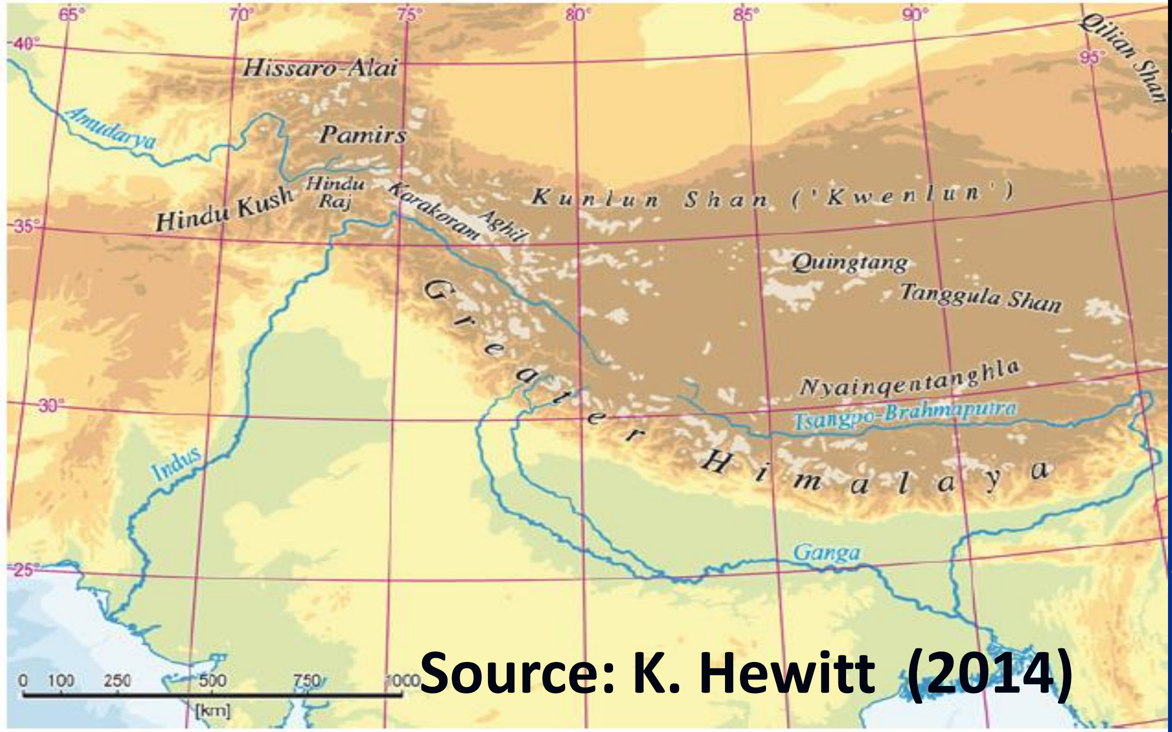

Source: K. Hewitt (2014)

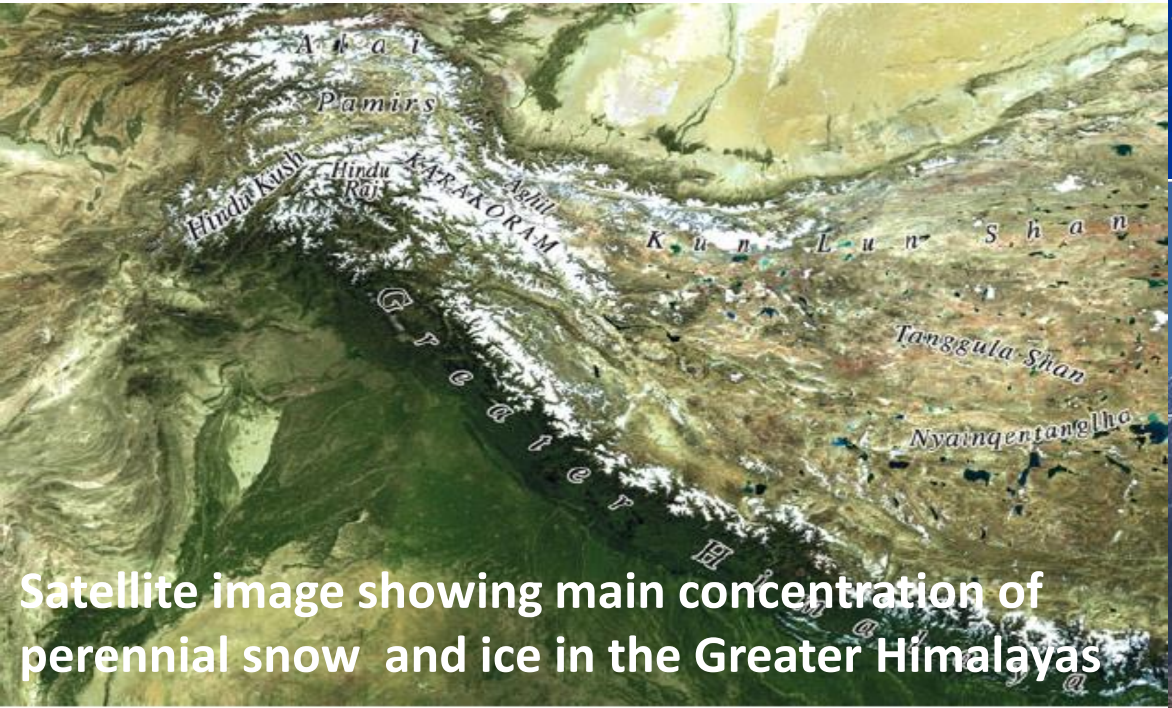

Satellite image showing main concentration of perennial snow and ice in the Greater Himalayas

High Asia

The Greater Himalayan Region:
Major river systems, Karakoram & other main mountain ranges with concentration of glaciers.

Karakoram: Extent & development of high mountain topography. Located in Southwest central part of High Asia

The Hindu Kush

Greater & Lesser Himalaya

Tibetan Plateau

The High Asian Cryosphere

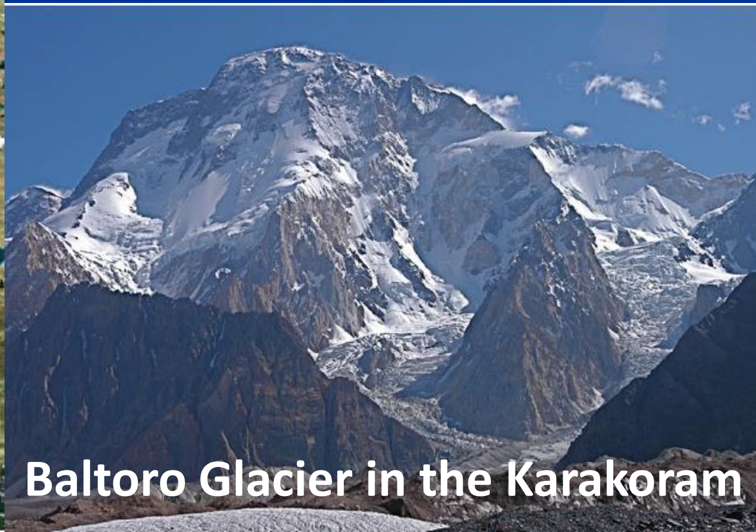

Baltoro Glacier in the Karakoram

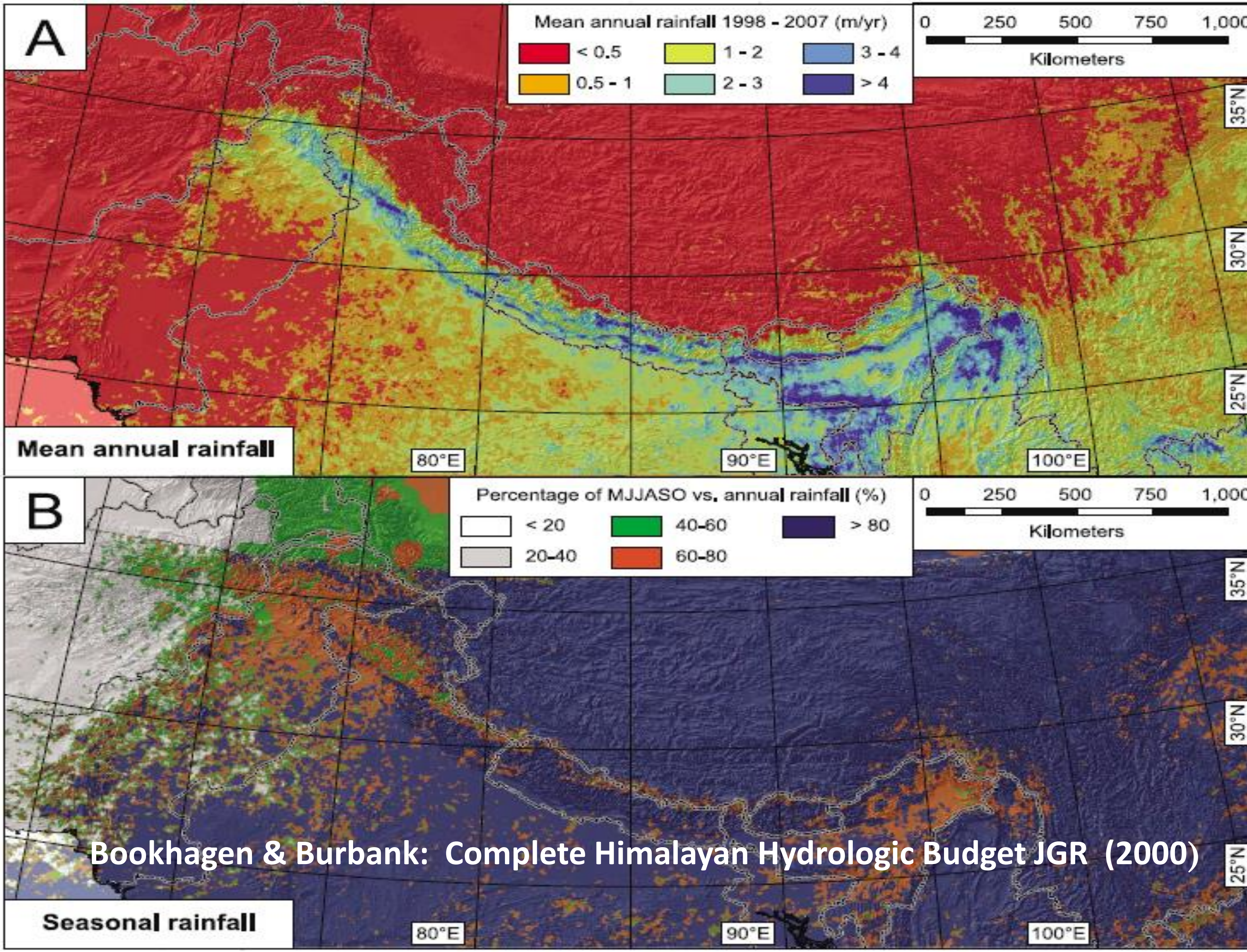

Bookhagen & Burbank: Complete Himalayan Hydrologic Budget JGR (2000)

Bhutiani et al. 2007: Significant rise in surface air temperatures over the Northwest Himalayan region by about 1.6°C during the last century, with winters warming at a faster rate.

SML - SHIMLA LH - LEH GMG - GULMERG HDT - HADDAN TAJ
SLG - SOLANG KZN - KANZALWAN PTS - PATSEO BHG - BAHANG
DHD - DHUNDI SGR - SRINAGAR

Station	Season→	Winter $b \times 100$	Monsoon $b \times 100$	Annual $b \times 100$
Shimla	Mean maximum	2.6*	2.8*	2.4*
	Mean minimum	1.0*	−0.01	0.5
	Average annual	1.8*	1.5*	2.0*
	Mean maximum	1.1*	0.2	0.5
Srinagar	Mean minimum	1.2*	0.2	1.0*
	Average annual	1.1*	0.2	0.8*
	Mean maximum	1.3*	1.0*	1.7*
Leh	Mean minimum	0.4*	1.1*	1.3*
	Average annual	0.6*	1.1*	1.6*
	Mean maximum	1.7*	1.3*	1.6*
NW-Himalaya	Mean minimum	1.7*	0.4*	1.1*
	Average annual	1.7*	0.9*	1.6*

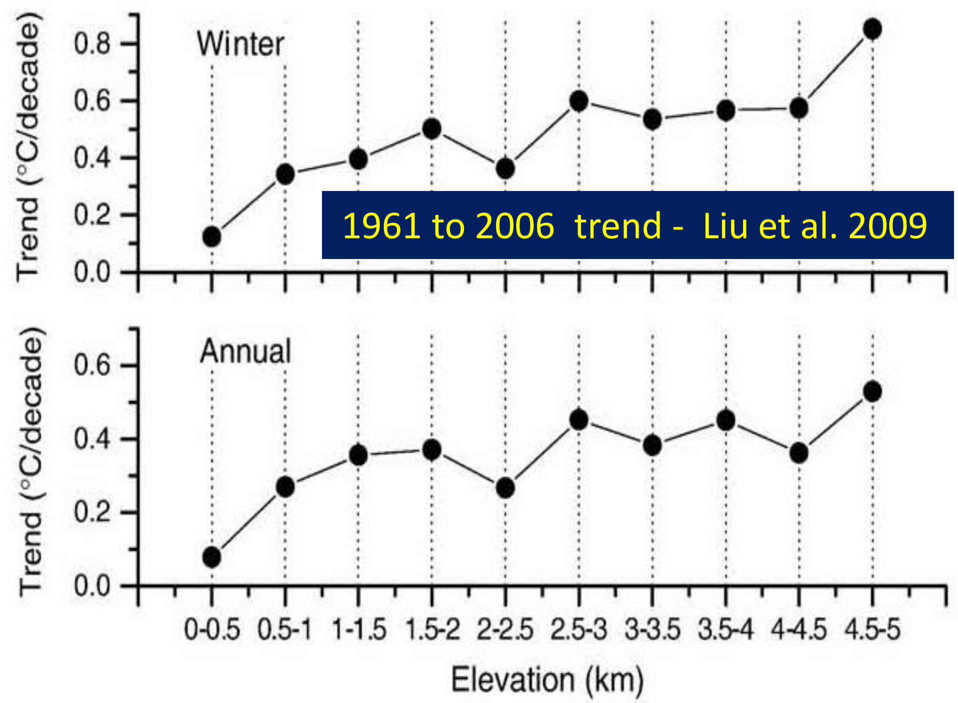

Elevation dependency of surface air temperature trends over the Tibetan Plateau & its surroundings - Liu et al. (2009), Shrestha et al. 1999

0.5° C per decade at higher elevations (> 2000 m)
0.2° C per decade for lower elevations (< 500 m)

The State and Fate of Himalayan Glaciers

T. Bolch,[1,2]* A. Kulkarni,[3] A. Kääb,[4] C. Huggel,[1,5] F. Paul,[1] J. G. Cogley,[6] H. Frey,[1,5] J. S. Kargel,[7] K. Fujita,[8] M. Scheel,[1,5] S. Bajracharya,[9] M. Stoffel[5,10]

Himalayan glaciers are a focus of public and scientific debate. Prevailing uncertainties are of major concern because some projections of their future have serious implications for water resources. Most Himalayan glaciers are losing mass at rates similar to glaciers elsewhere, except for emerging indications of stability or mass gain in the Karakoram. A poor understanding of the processes affecting them, combined with the diversity of climatic conditions and the extremes of topographical relief within the region, makes projections speculative. Nevertheless, it is unlikely that dramatic changes in total runoff will occur soon, although continuing shrinkage outside the Karakoram will increase the seasonality of runoff, affect irrigation and hydropower, and alter hazards.

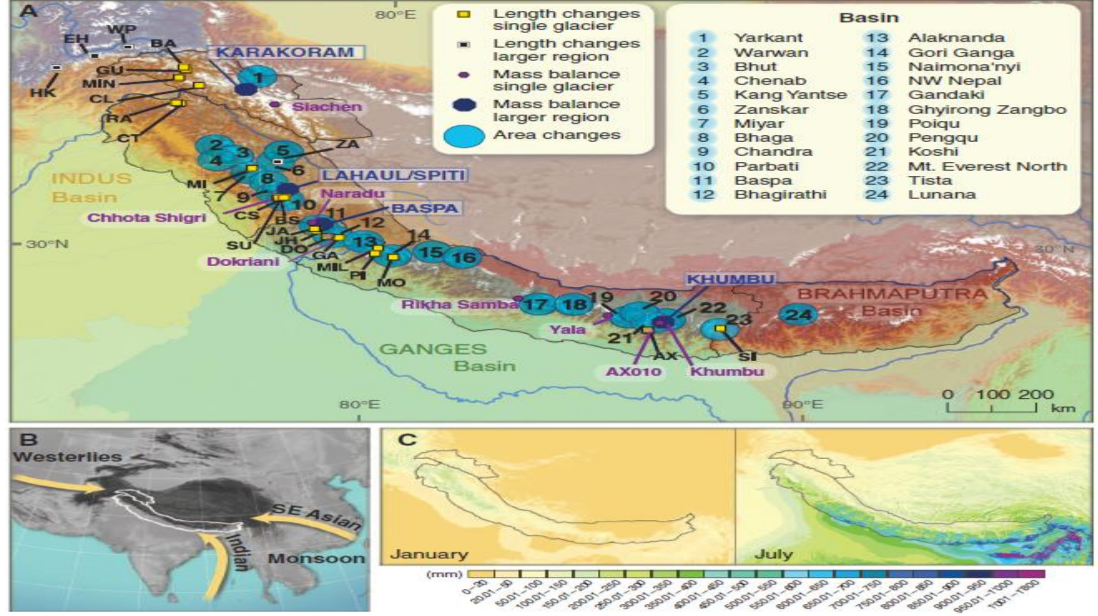

Fig. 1. **(A)** Map of the Karakoram and Himalaya showing the major river basins and the locations of measured rates of change in area and of a sample of glacier length change and mass budget measurements (4) (tables S3, S5, and S6). **(B)** Main wind systems. **(C)** Mean precipitation in January and July. [Source: (9)]

Slight mass gain of Karakoram glaciers in the early twenty-first century

Julie Gardelle[1]*, Etienne Berthier[2] and Yves Arnaud[3]

Assessments of the state of health of Hindu-Kush–Karakoram–Himalaya glaciers and their contribution to regional hydrology and global sea-level rise suffer from a severe lack of observations[1]. The globally averaged mass balance of glaciers and ice caps is negative[1–3]. An anomalous gain of mass has been suggested for the Karakoram glaciers[2,4–6], but was not confirmed by recent estimates of mass balance. Furthermore, numerous glacier surges in the region that lead to changes in glacier length and velocity[7–11] complicate the interpretation of the available observations. Here, we calculate the regional mass balance of glaciers in the central Karakoram between 1999 and 2008, based on the difference between two digital elevation models. We find a highly heterogeneous spatial pattern of changes in glacier elevation, which shows that ice thinning and ablation at high rates can occur on debris-covered glacier tongues. The regional mass balance is just positive at $+0.11 \pm 0.22\,\mathrm{m\,yr^{-1}}$ water equivalent and in agreement with the observed reduction of river runoff that originates in this area[12]. Our measurements confirm an anomalous mass balance in the Karakoram region and indicate that the contribution of Karakoram glaciers to sea-level rise was $-0.01\,\mathrm{mm\,yr^{-1}}$ for the period from 1999 to 2008, 0.05 mm yr^{-1} lower than suggested before[13].

Snowfall less sensitive to warming in Karakoram than in Himalayas due to a unique seasonal cycle **Kapnick et al. 2014**

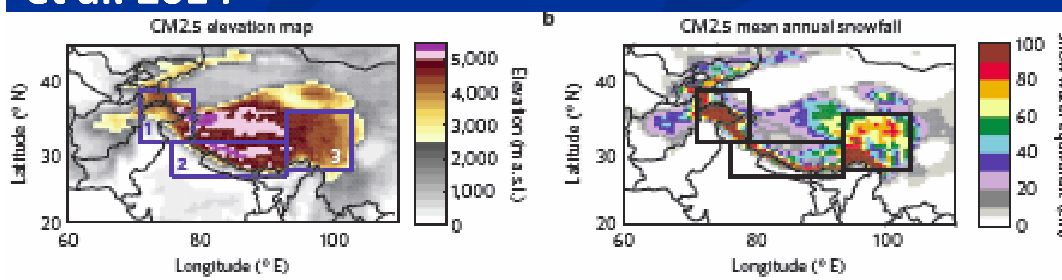

The Karakoram seasonal cycle is dominated by non-monsoonal winter precipitation, which uniquely protects it from reductions in annual snowfall under climate warming over the twenty-first century. The simulations show that climate change signals are detectable only with long and continuous records, and at specific elevations. Kapnick et al. (2014) suggest a meteorological mechanism for regional differences in the glacier response to climate warming.

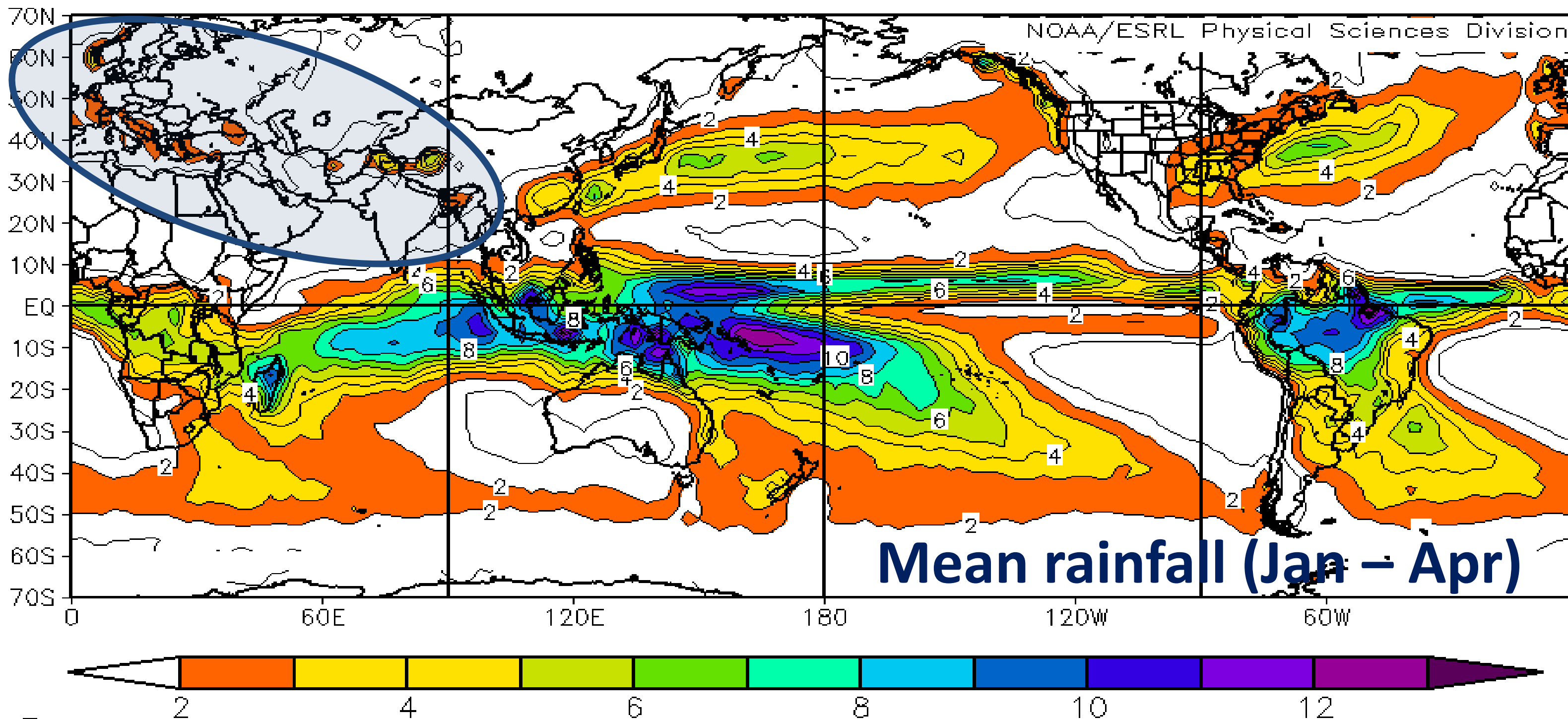
NOAA/ESRL Physical Sciences Division
Mean rainfall (Jan – Apr)
70N
60N
50N
40N
30N
20N
10N
EQ
10S
20S
30S
40S
50S
60S
70S
0
60E
120E
180
120W
60W
0
2
4
6
8
10
12

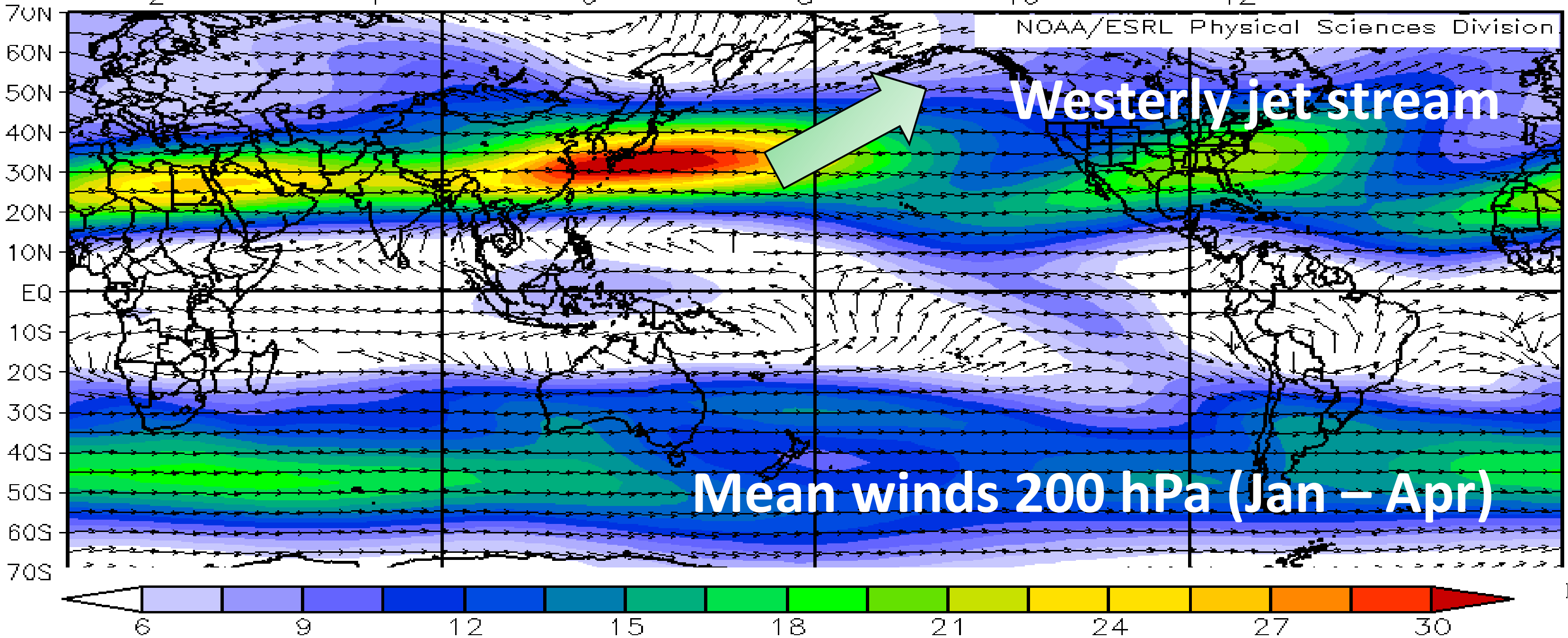
NOAA/ESRL Physical Sciences Division
Westerly jet stream
Mean winds 200 hPa (Jan – Apr)
70N
60N
50N
40N
30N
20N
10N
EQ
10S
20S
30S
40S
50S
60S
70S
6
9
12
15
18
21
24
27
30

Winter and early spring (Dec-Jan-Feb-Mar-Apr)

Mean seasonal (DJFMA) precipitation (mm day^{-1})

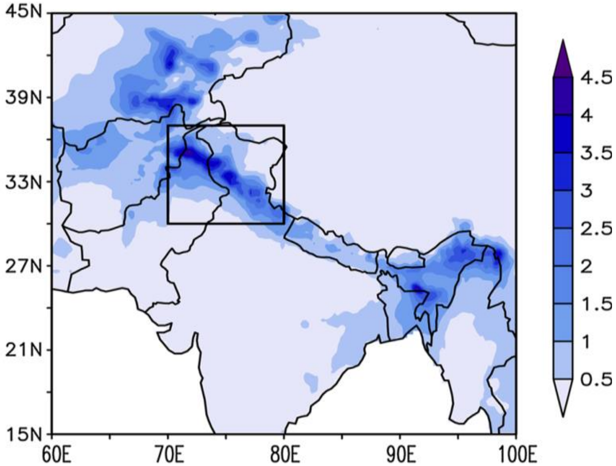

APHRODITE precip (1951-2014)

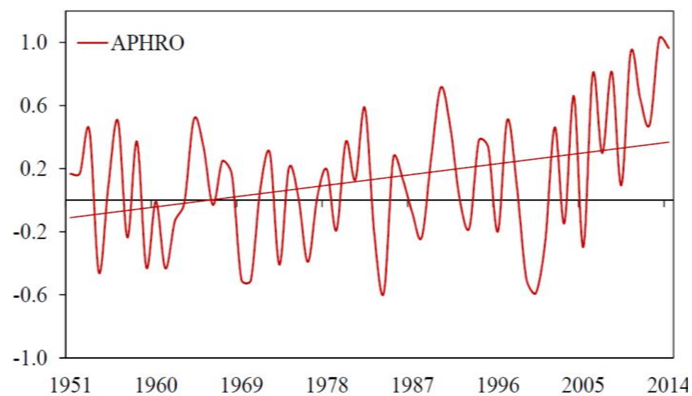

Spatial map of linear trend in DJFMA precipitation

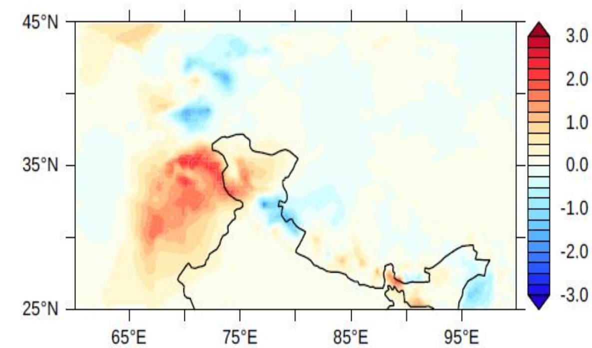

Large orographic gradients of WH

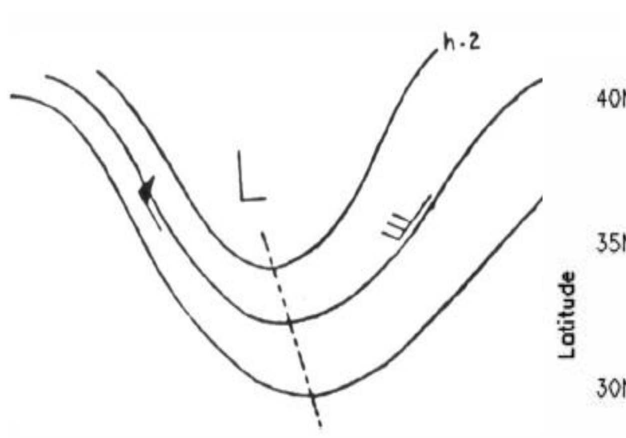

Schematic representation of asymmetric upper air trough (Pisharoty and Desai, 1956)

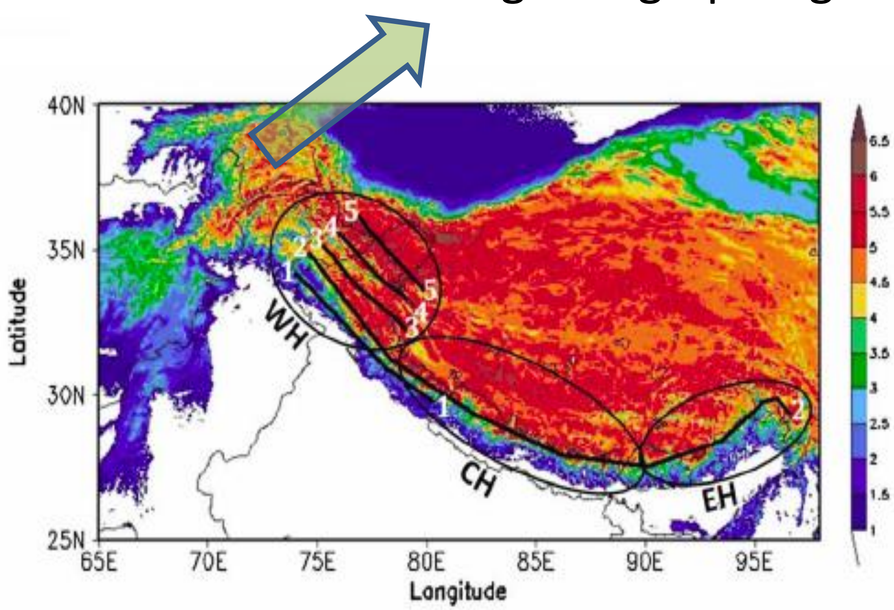

Schematic representation of cascading Himalayan mountains with topographic height (km, shaded).

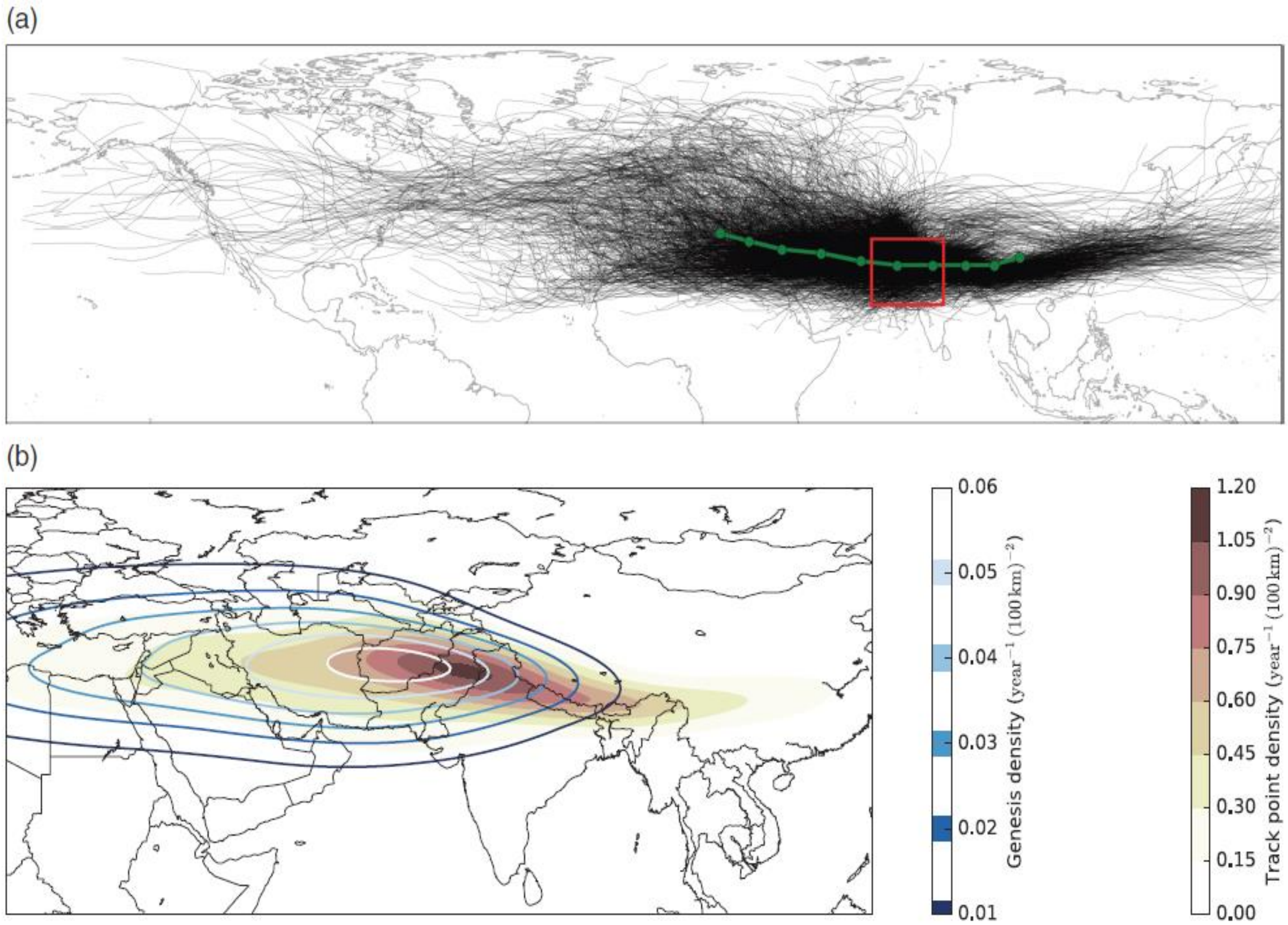

Kieran Hunt et al. (2018) QJRMS

Representation of some bulk spatial statistics of WD tracks (a) All 3090 tracks found in ERA-Interim (1979-2015) (b) Contour plots of genesis (lines) and track point (solid) densities with units of year^{-1} (100 km)$^{-2}$. In (a), the red box indicates the box through which the tracks must pass to be considered; the segmented green track indicates the mean position for 5 days either side of maximum intensity

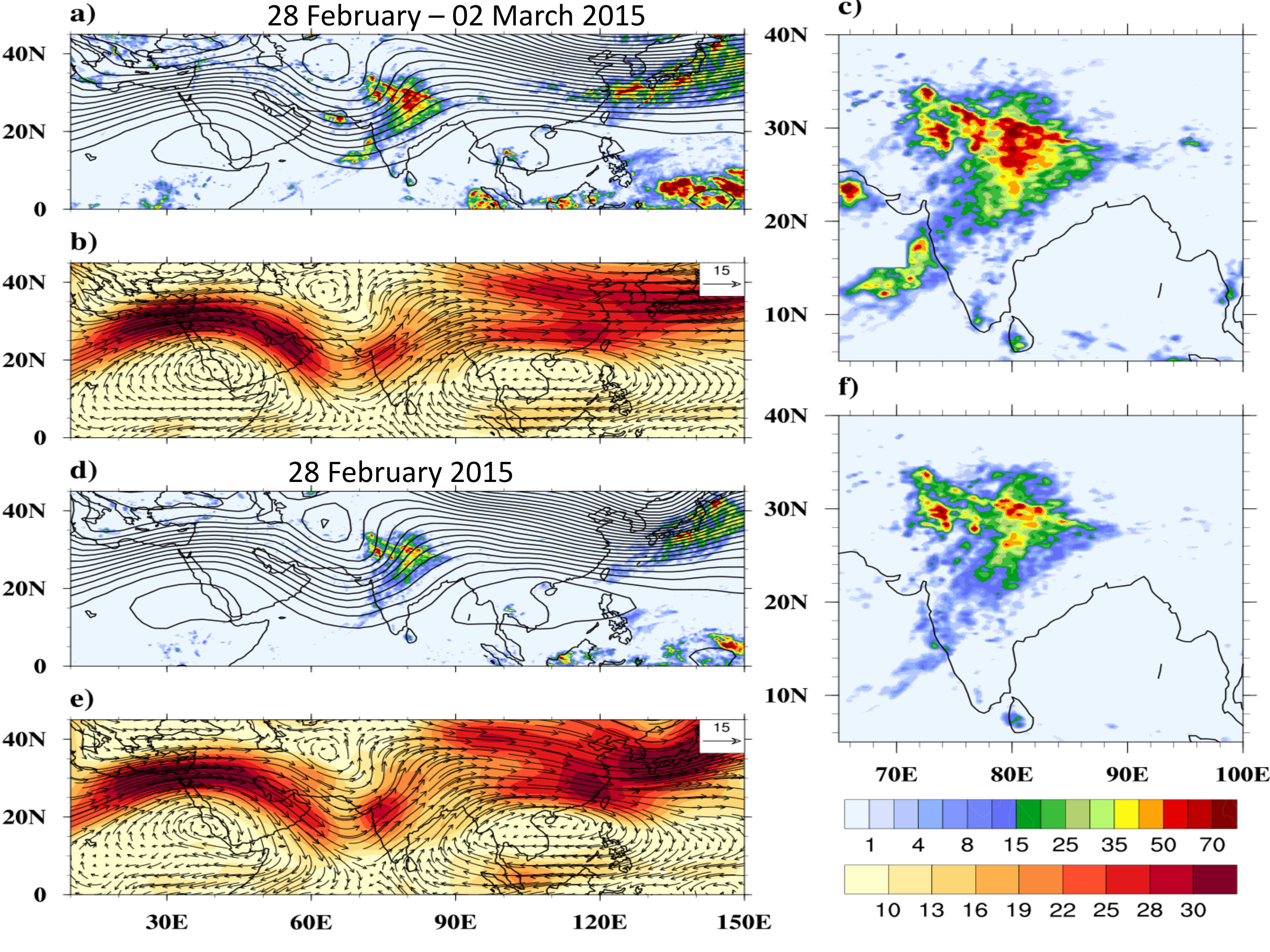

a)
28 February – 02 March 2015
b)
15
c)
d)
28 February 2015
e)
15
f)
40N
30N
20N
10N
0
30E
60E
90E
120E
150E
70E
80E
90E
100E
1
4
8
15
25
35
50
70
10
13
16
19
22
25
28
30

Adapted from Cannon et al. 2015

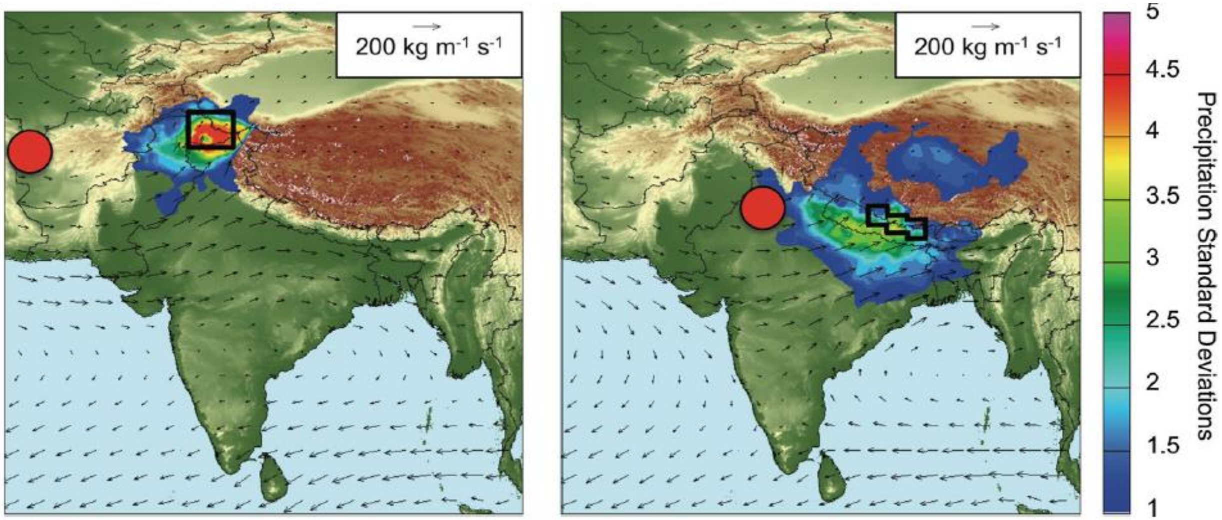

Red circle: 200 hPa geopotential height anomaly centre during heavy precipitation (lag 0) over Karakoram (left), Central (right)

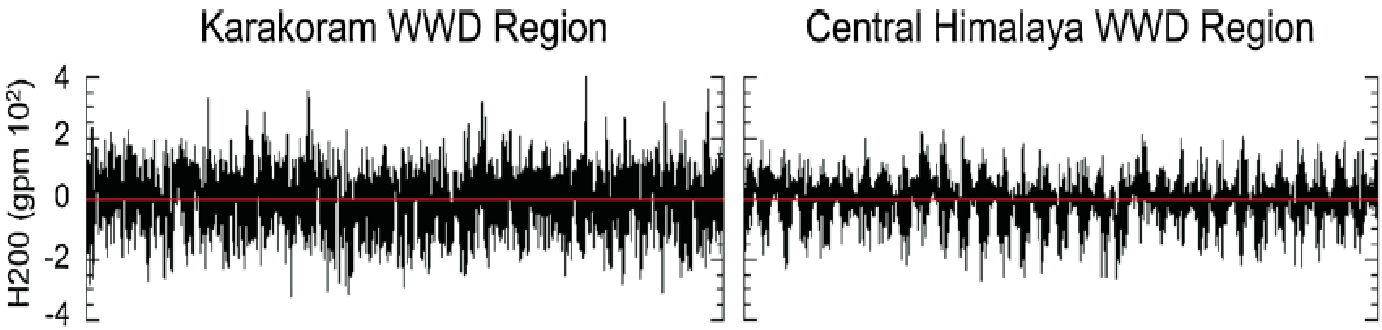

200 hPa Geopotential height anomalies time-series (1979-2010) around the negative anomalies during heavy precip events (day 0) over KH and CH

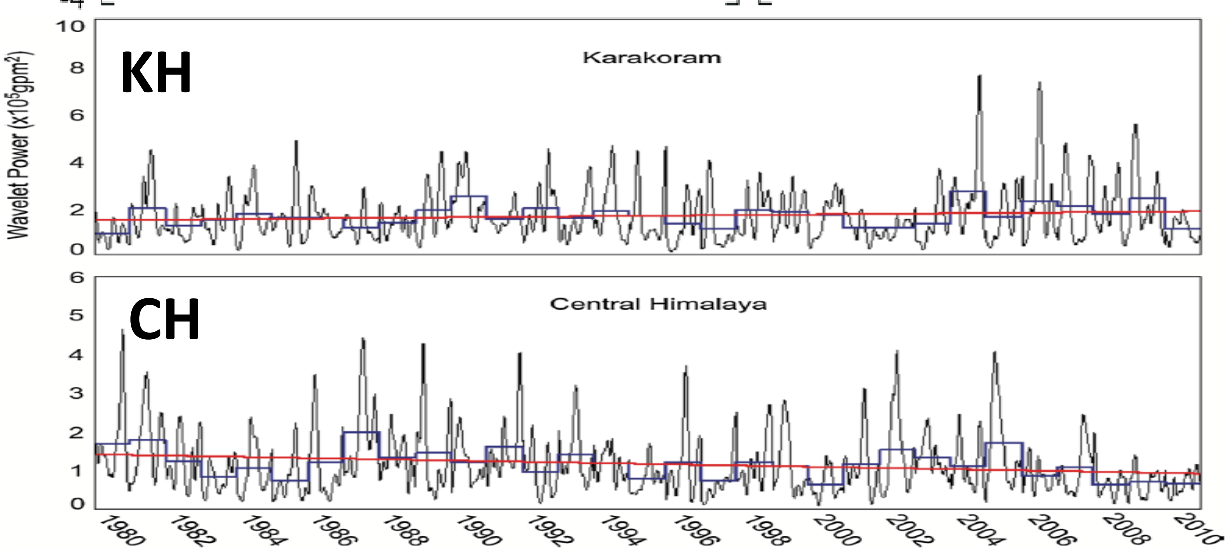

KH: Increasing trend of power - strengthening of WD

CH: Decreasing trend of power - Weakening of WD

Increasing trend in the amplitude variations of WDs

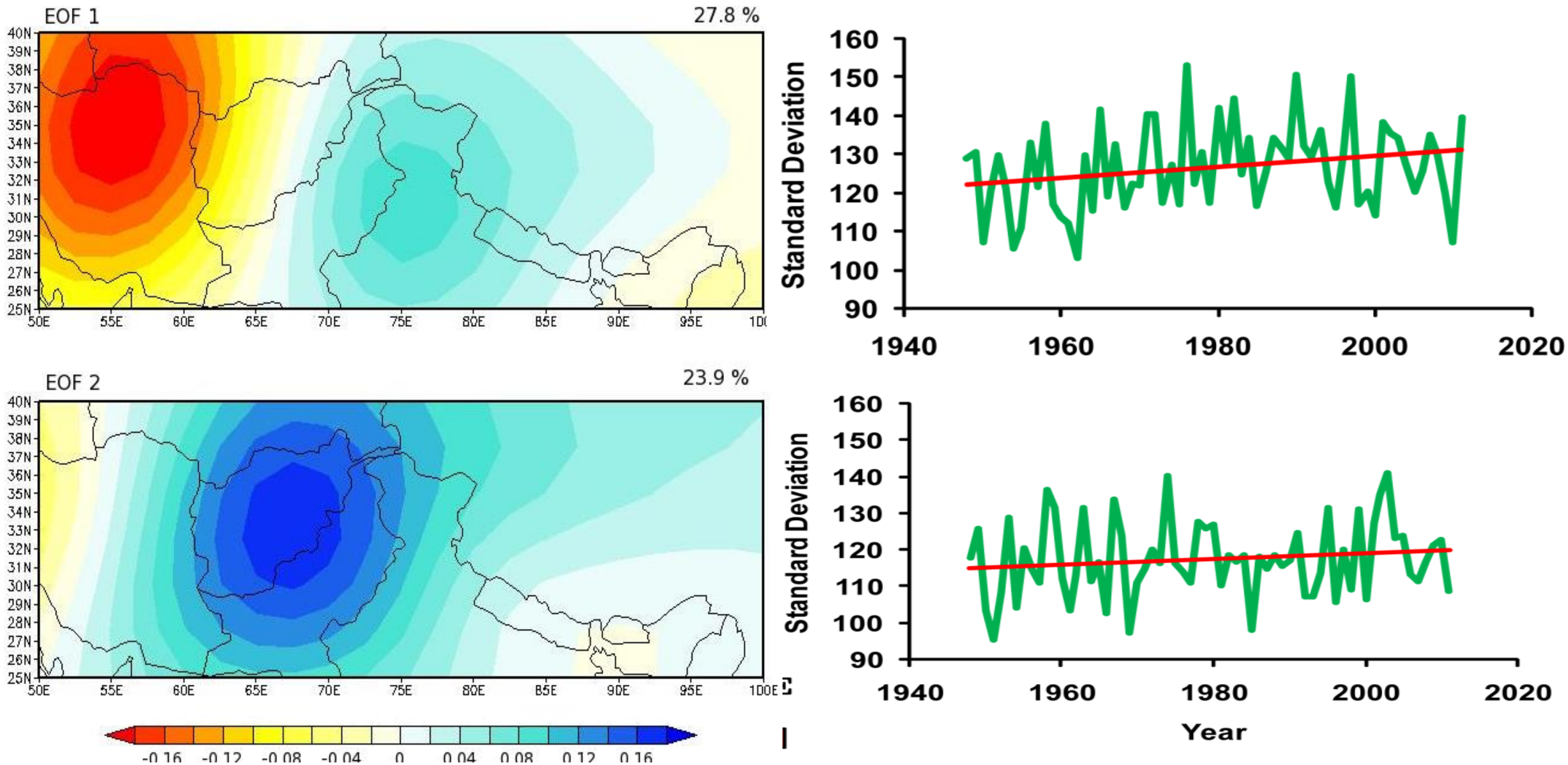

Latitude weighted EOF/PC analysis of daily high-frequency geopotential height anomalies (500 hPa) DJFMA season (1948 – 2011). Time series show standard deviation of PCs computed for each DJFMA season

Madhura et al. 2014

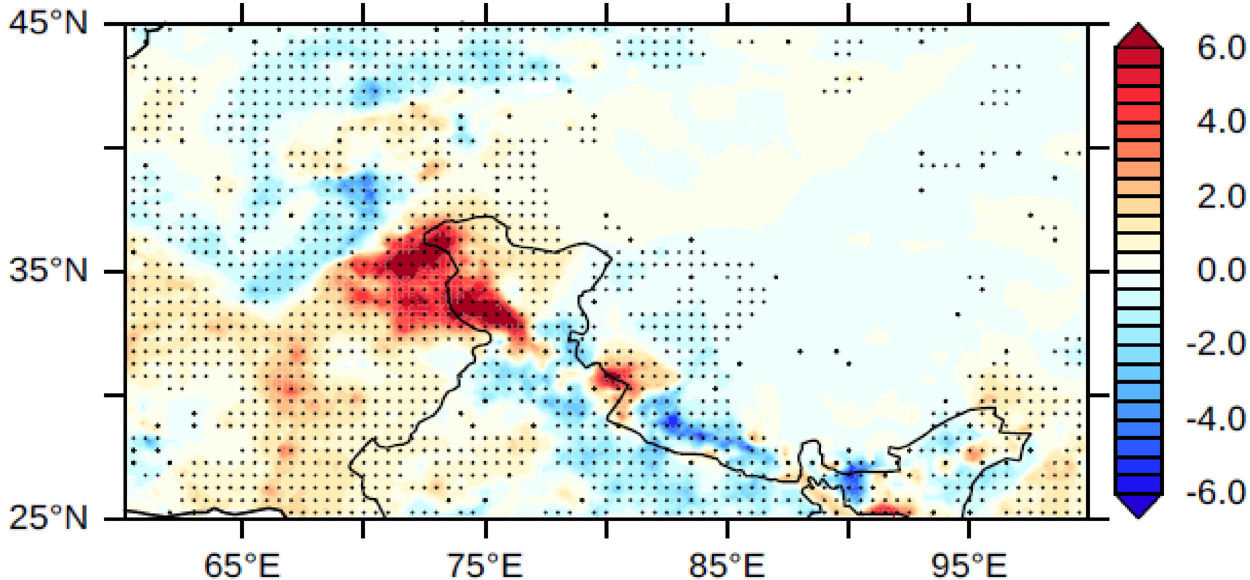

Spatial map of trend in daily precipitation (DJFMA) exceeding the 90th percentile during 1951-2007 (APHRODITE)

Krishnan et al. (2018)

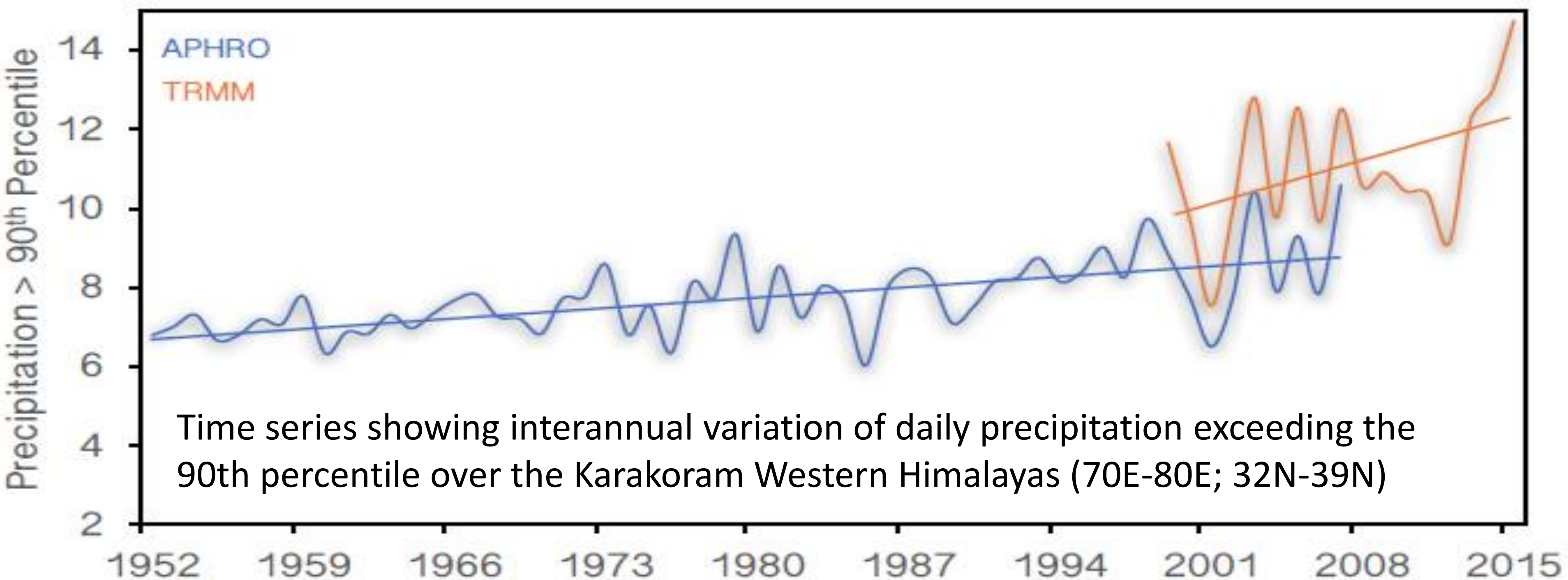

Time series showing interannual variation of daily precipitation exceeding the 90th percentile over the Karakoram Western Himalayas (70E-80E; 32N-39N)

LMDZ grid setup for CORDEX South Asia (shaded region has grid-size < 35 km)

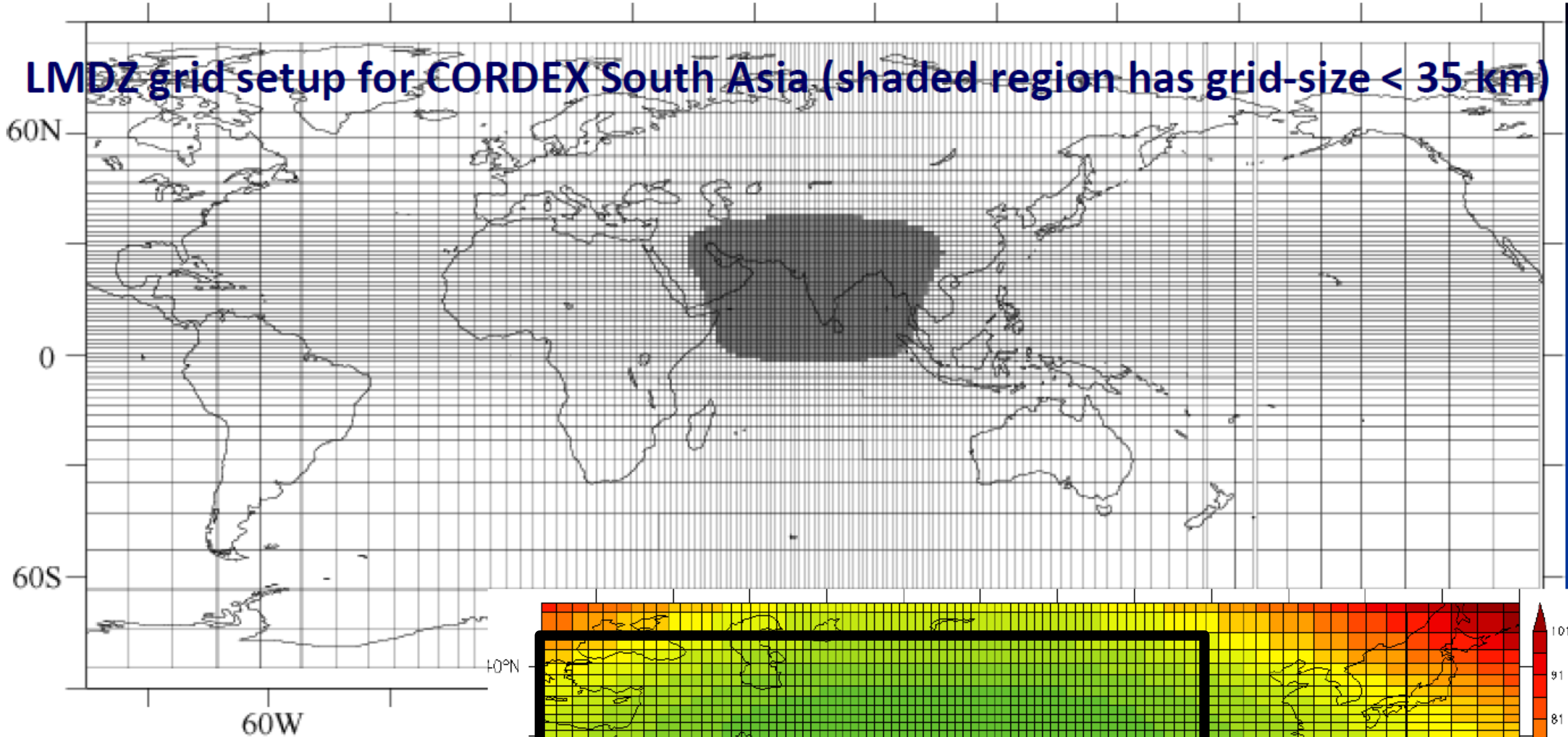

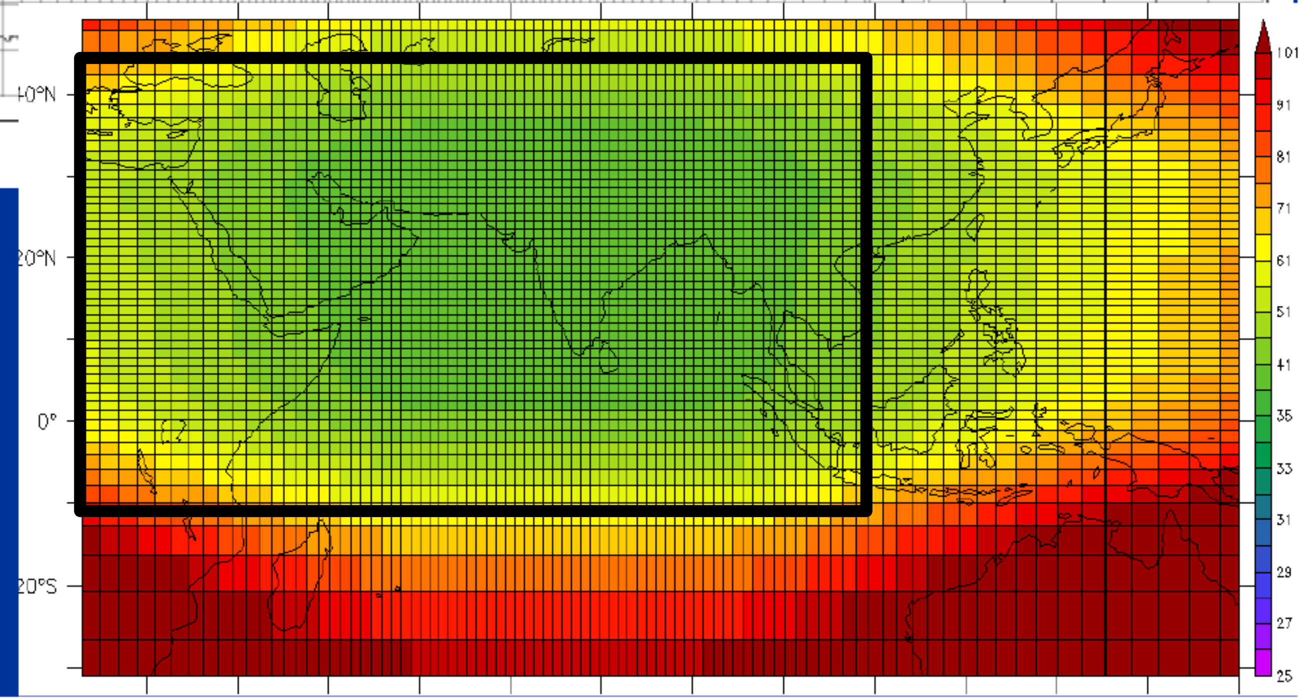

LMDZ global atmospheric model: Variable resolution with zooming capability

Source: Sabin, CCCR, IITM

High-resolution (~ 35 km) modeling of **climate change over S.Asia**

Historical (1886-2005):

Includes natural and anthropogenic (GHG, aerosols, land cover etc) climate forcing during the historical period (1886 – 2005) ~ 120 years

Historical Natural (1886 – 2005):

Includes only natural climate forcing during the historical period (1886– 2005) ~ 120 yrs

RCP 4.5 scenario (2006-2100) ~ 95 years:

Future projection run which includes both natural and anthropogenic forcing based on the IPCC AR5 RCP4.5 climate scenario. The evolution of GHG and anthropogenic aerosols in RCP4.5 produces a global radiative forcing of + 4.5 W m^{-2} by 2100

Runs performed on PRITHVI, CCCR-IITM

CO2 concentration in future IPCC AR5 scenarios

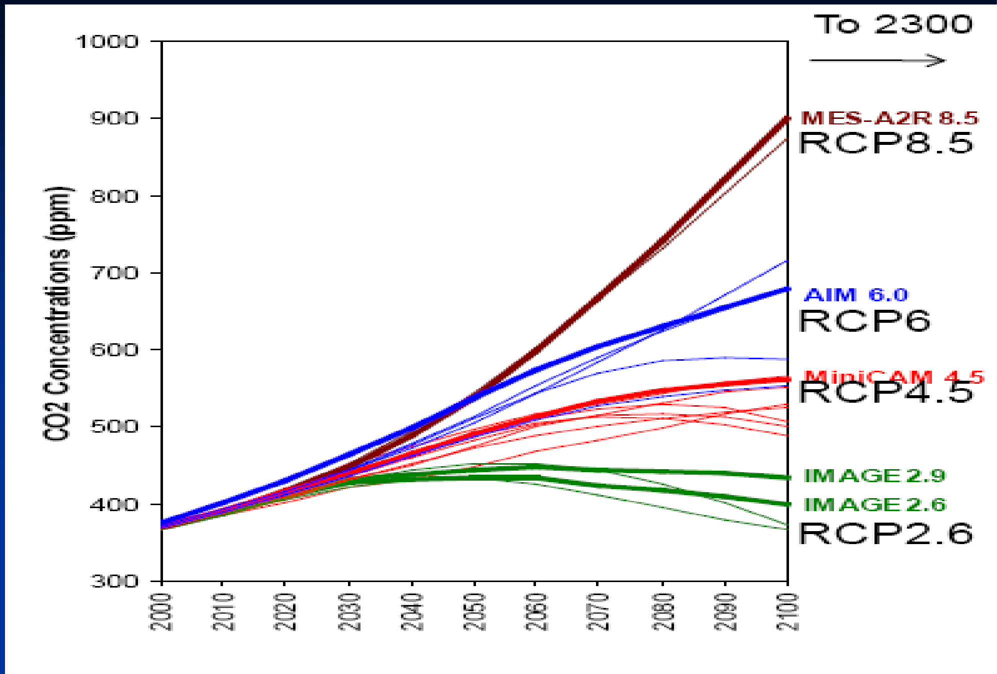

Aerosol distribution from IPSL ESM

INCA: INteraction with Chemistry and Aerosol

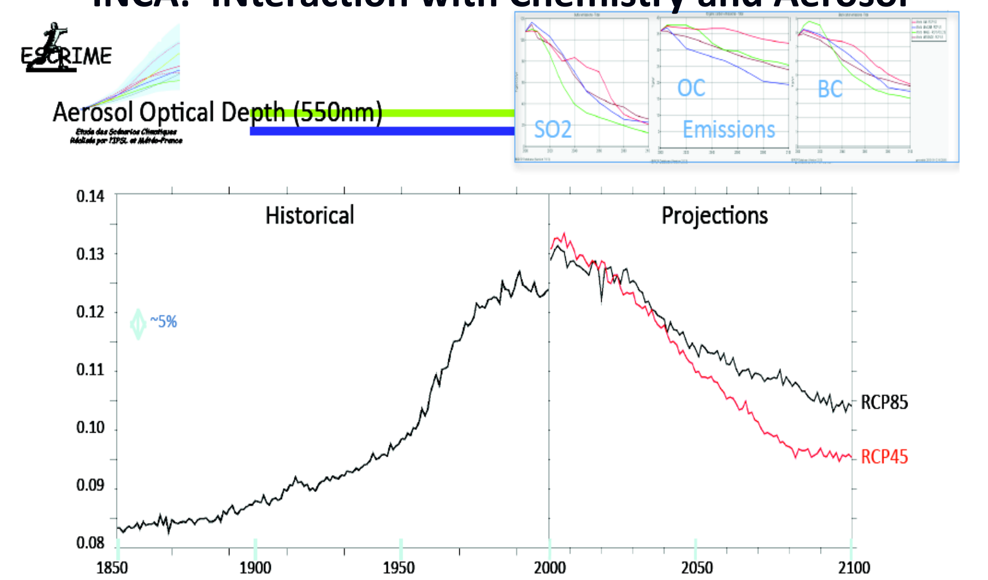

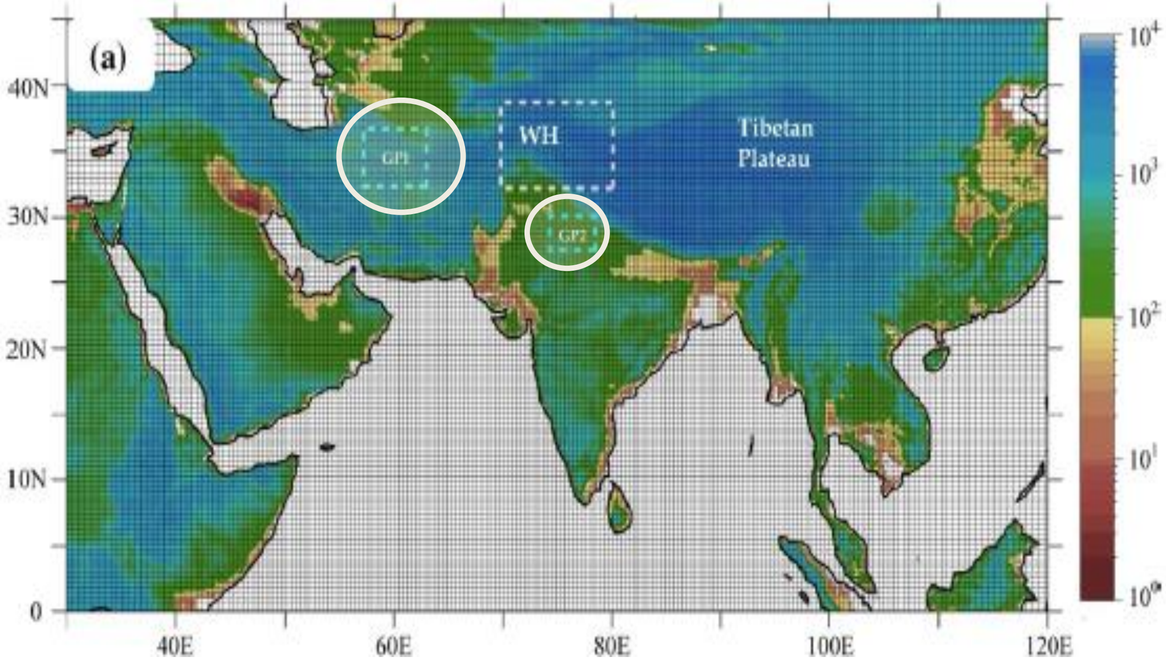

The LMDZ4 model horizontal grid and model topography (shaded; units in meters) and the domain of the Western Himalayas (WH, 70°E–80°E and 32°N–39°N). The boxes GP1 (58°E–62°E, 32°N–36°N) andGP2 (75°E–78°E, 28°N–30°N) correspond to centers of daily anomalies of geopotential height at 200 hPa influencing the lag-0 precipitation over the Western and Central Himalayas, respectively (Cannon et al. 2015)

Annual cycle of precipitation & temperature
Observations and Model (WH)

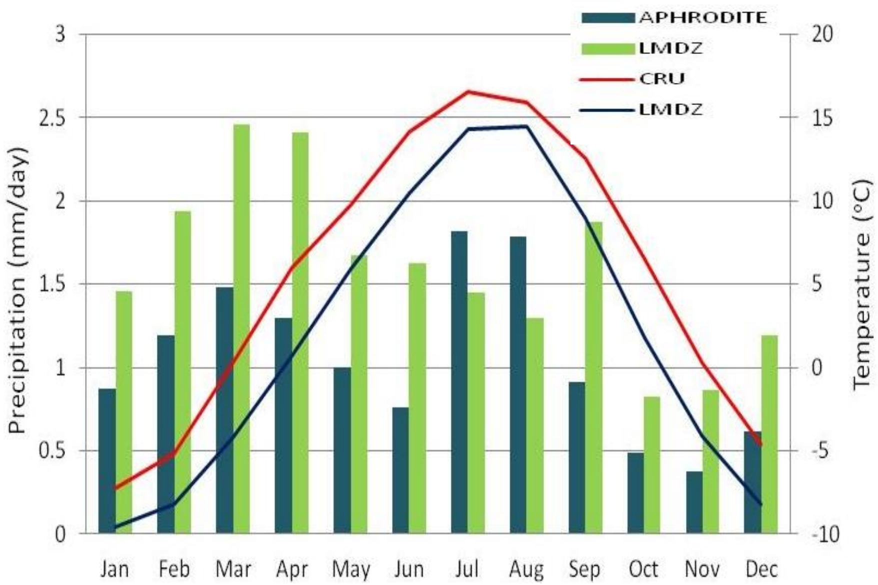

Annual cycle of snowfall (%) and rainfall (%)
Observations and Model (WH)

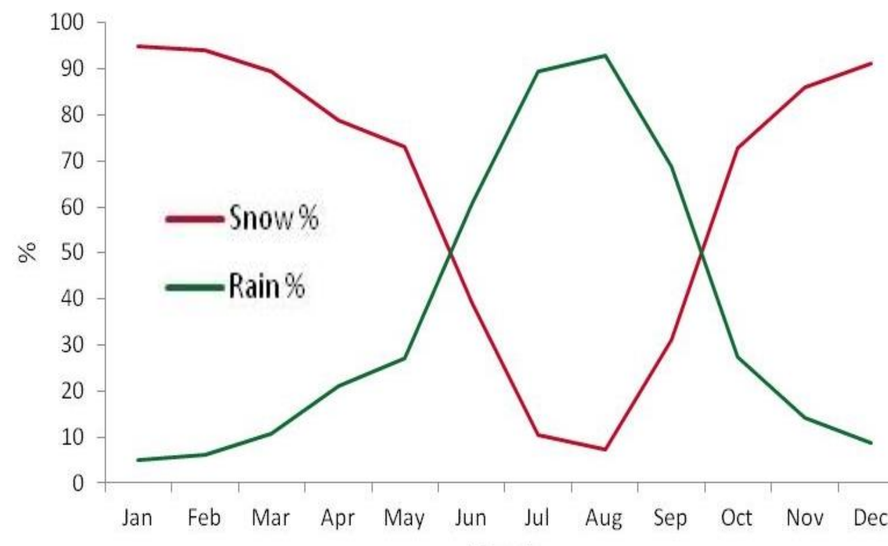

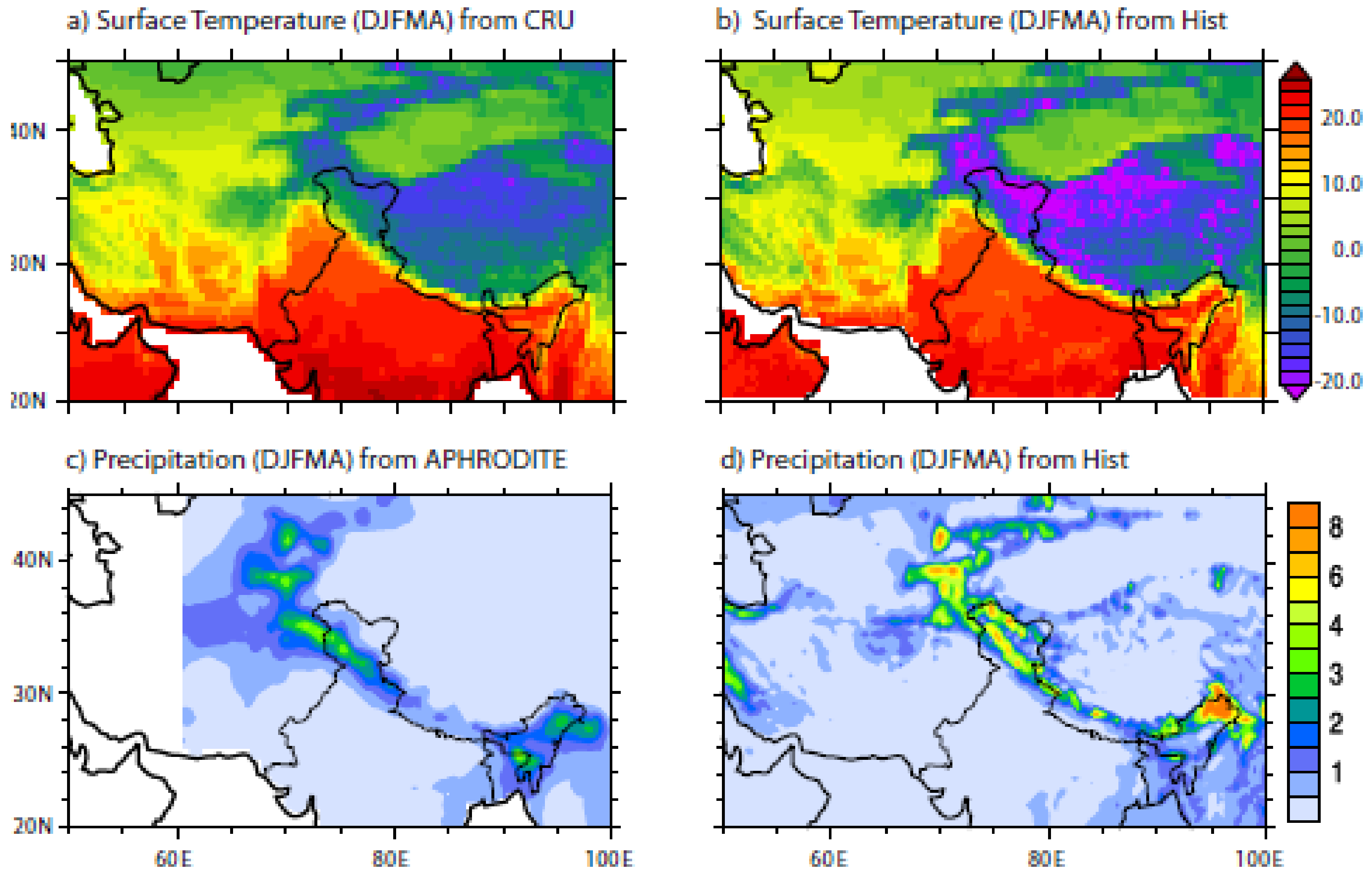

Spatial maps of DJFMA climatological surface air temperature (^{o}C) & precipitation (mm day^{-1}) from observations and model simulation (HIST)

Climatological mean horizontal winds at 200 hPa for the DJFMA months (a) ERA-Interim (b) HIST simulation. Shading denotes wind speed (m/s).

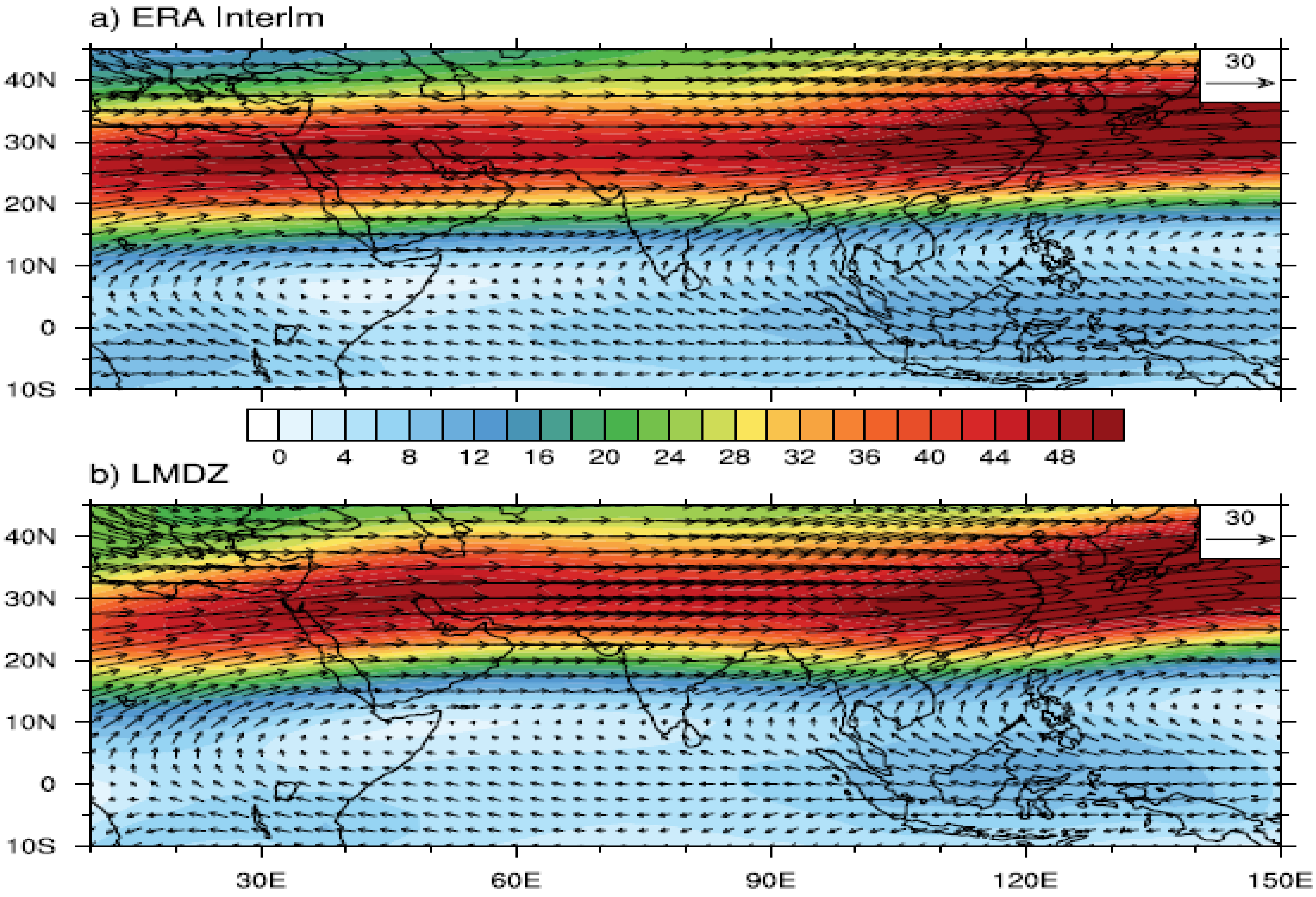

Spectral variance of daily zonal winds (m^2s^{-2}) at 200 hPa averaged over the region (40-80E, 25-35N) of the subtropical westerly jet

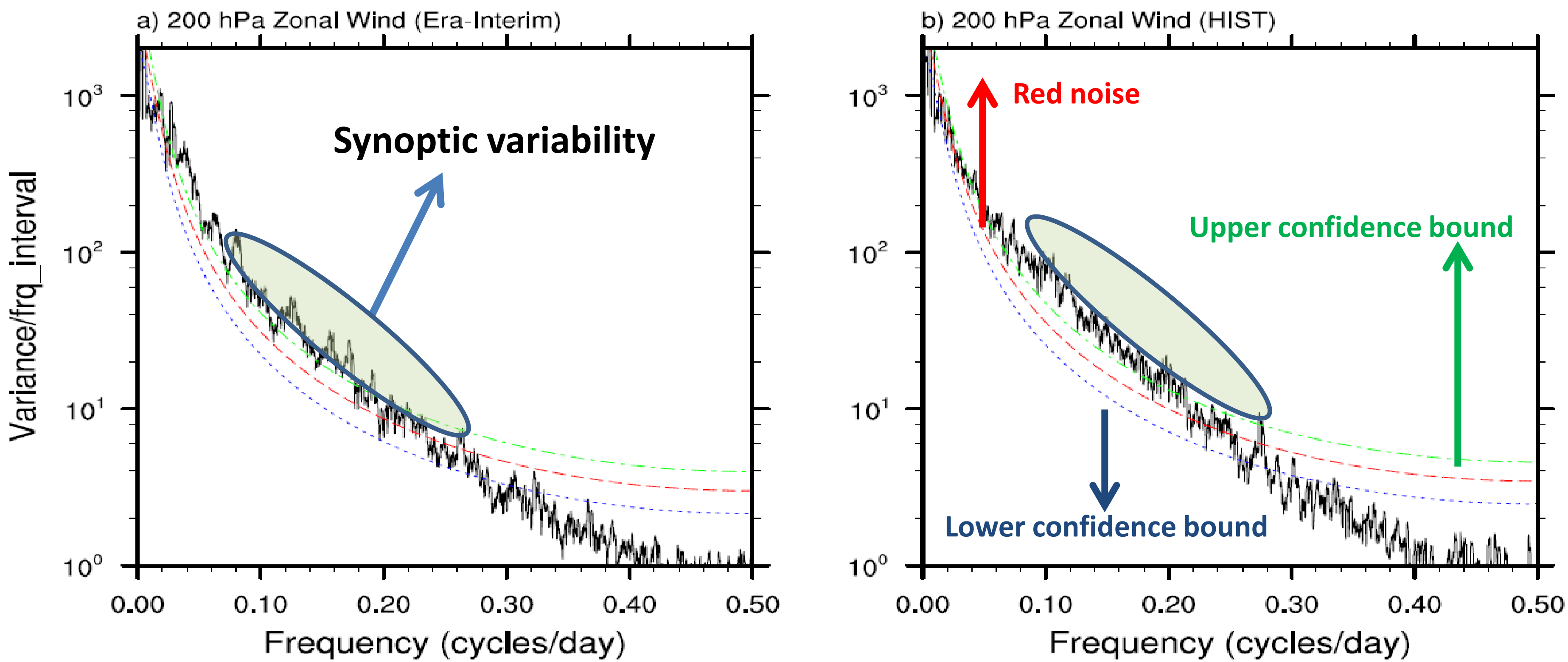

ERA-Interim **HIST simulation**

Synoptic variability: ~ 4 – 10 days

Krishnan et al. (2018)

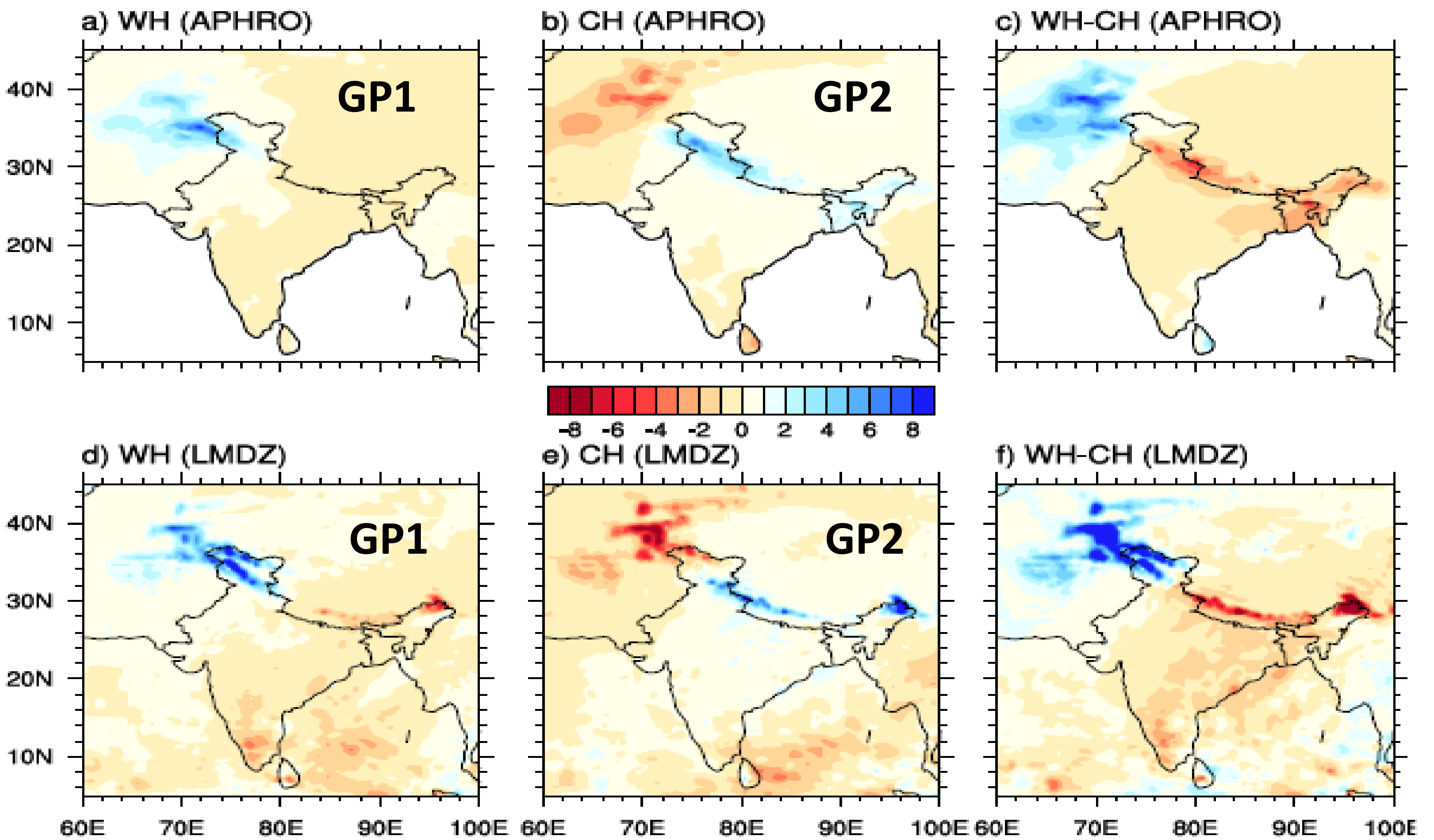

Composites of lag-0 precipitation anomalies (mm day^{-1}) over the WH and CH, associated with synoptic-scale WDs, constructed by taking the difference between the 15th percentile and 85th percentile of the 4-15 day band-pass filtered time-series of GP1 (for WH) and GP2 (for CH), respectively. This approach is similar to Cannon et al. (2015). (a-c) Anomaly composites [WH, CH and difference (WH-CH)] based on the APRHODITE precipitation dataset (d-f) Same as (a-c) except for HIST.

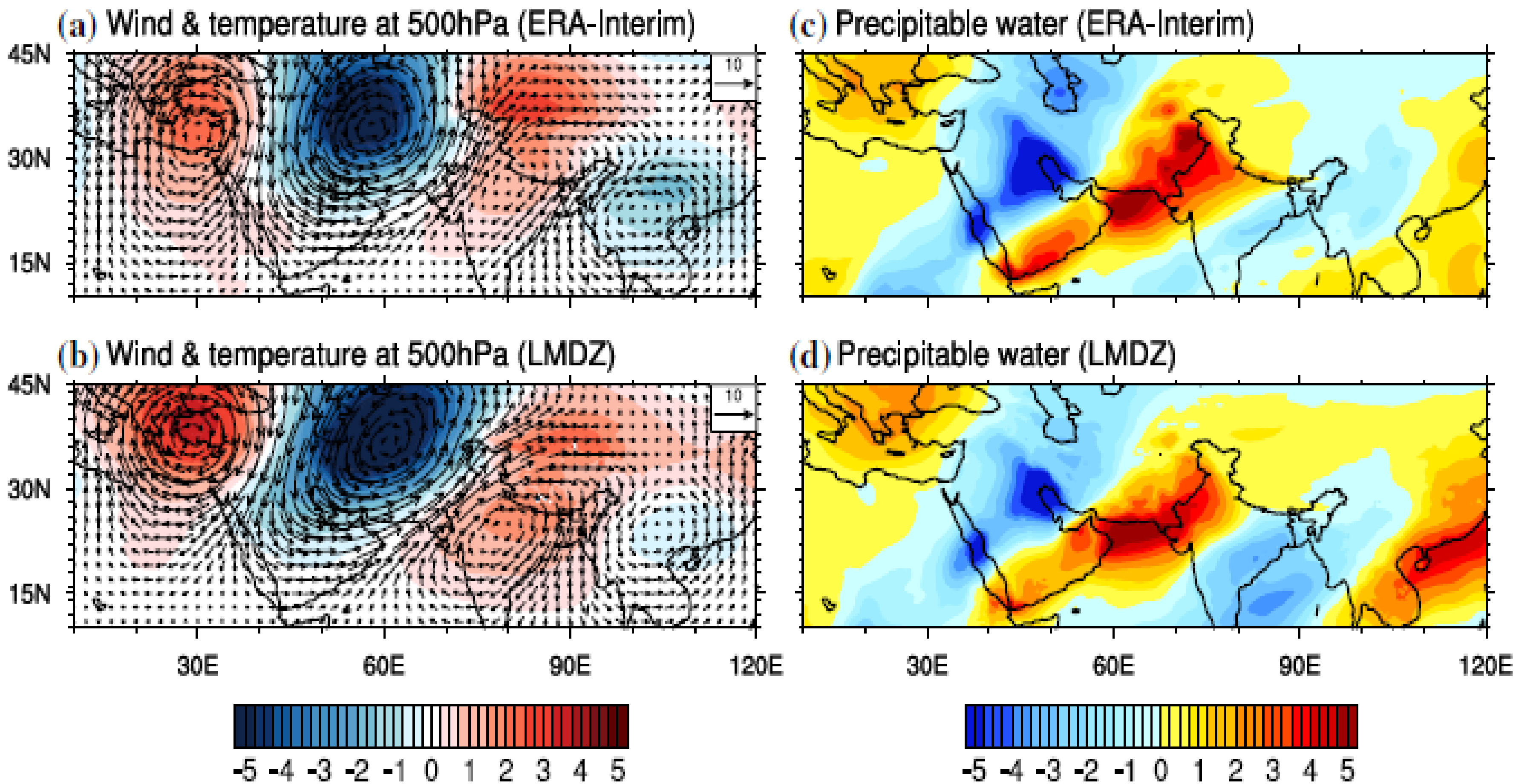

Composites of lag-0 anomalies of 500 hPa circulation and precipitable water associated with the synoptic scale WDs, constructed by taking the difference (15^{th} minus 85^{th}) percentiles of the 4-15 days band-pass filtered time-series of GP1 from ERA-Interim and HIST simulation

Krishnan et al. (2018)

Difference between HIST and NATURAL simulations (1951-2005): DJFMA Mean

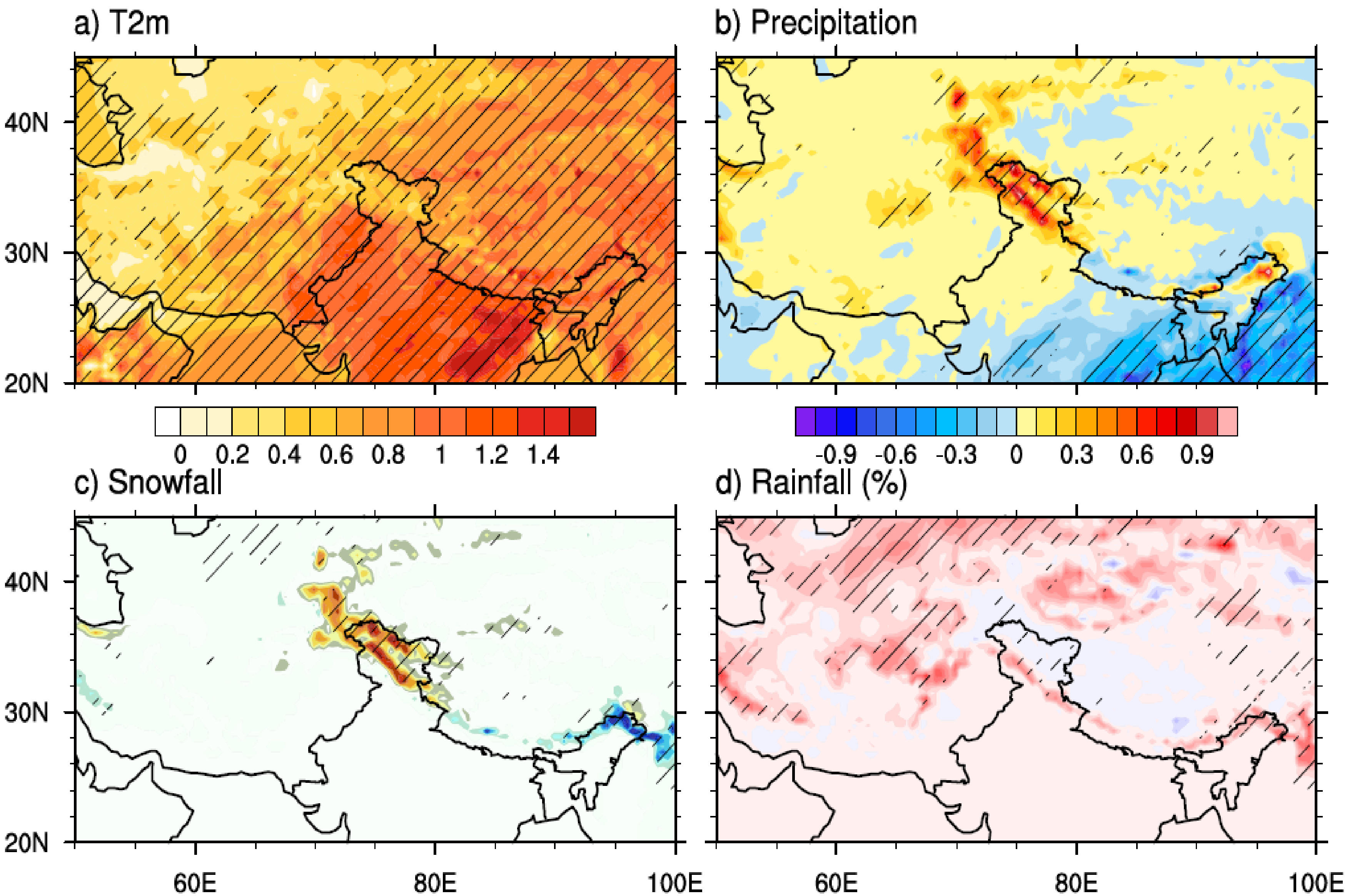

Spatial map of trend in daily precipitation (DJFMA) exceeding the 90th percentile

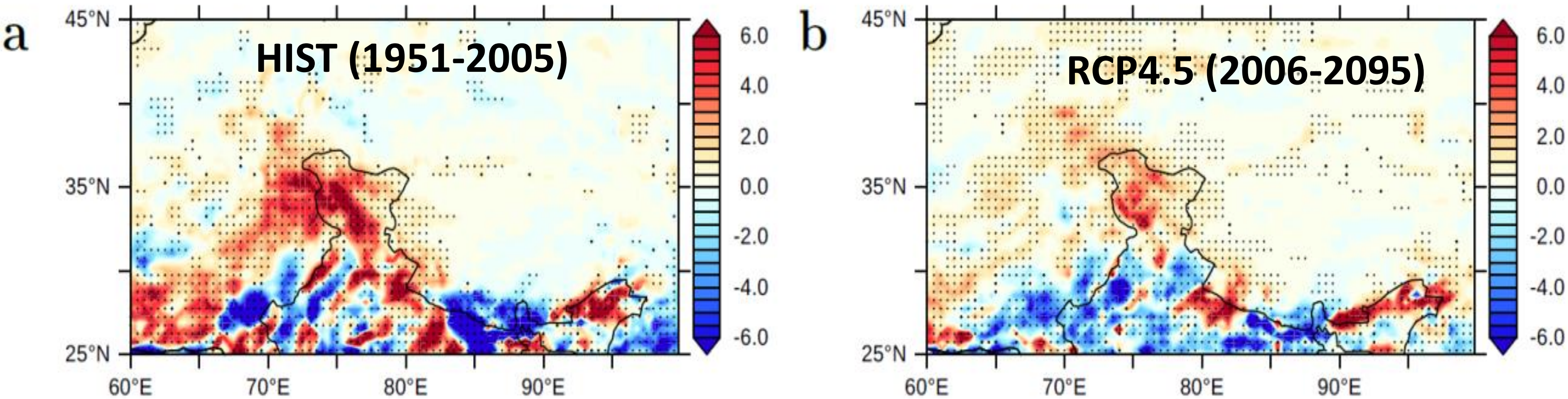

Time series showing interannual variation of daily precipitation exceeding the 90th percentile over the Karakoram Western Himalayas (70E-80E; 32N-39N) for HIST, HISTNAT & RCP4.5

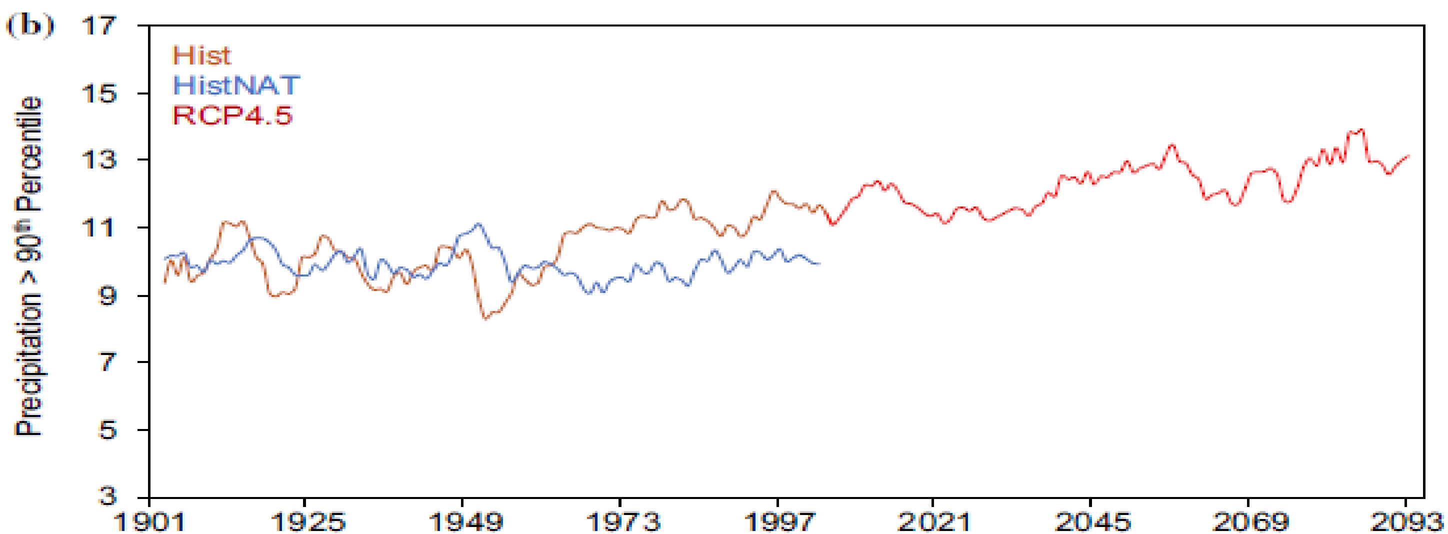

Time-series showing amplitude variations of WDs associated with precipitation over the Karakoram Himalayas

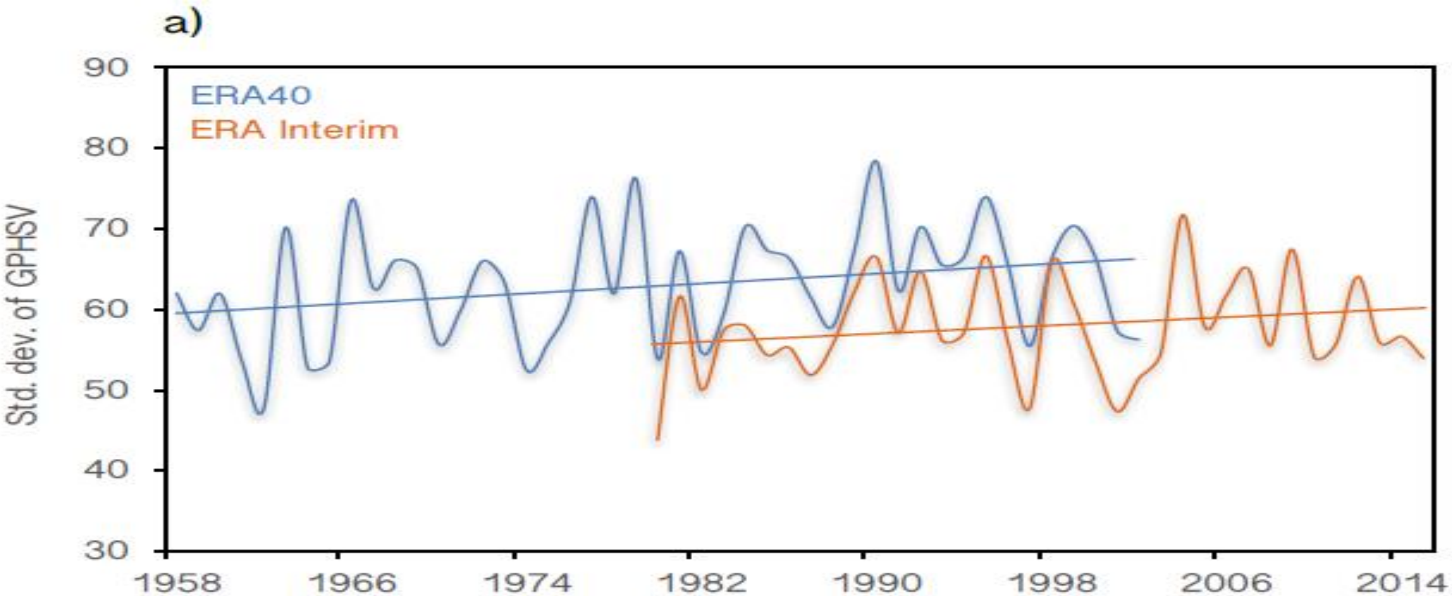

ERA 40 (1958-2002)

ERA-Interim (1979-2015)

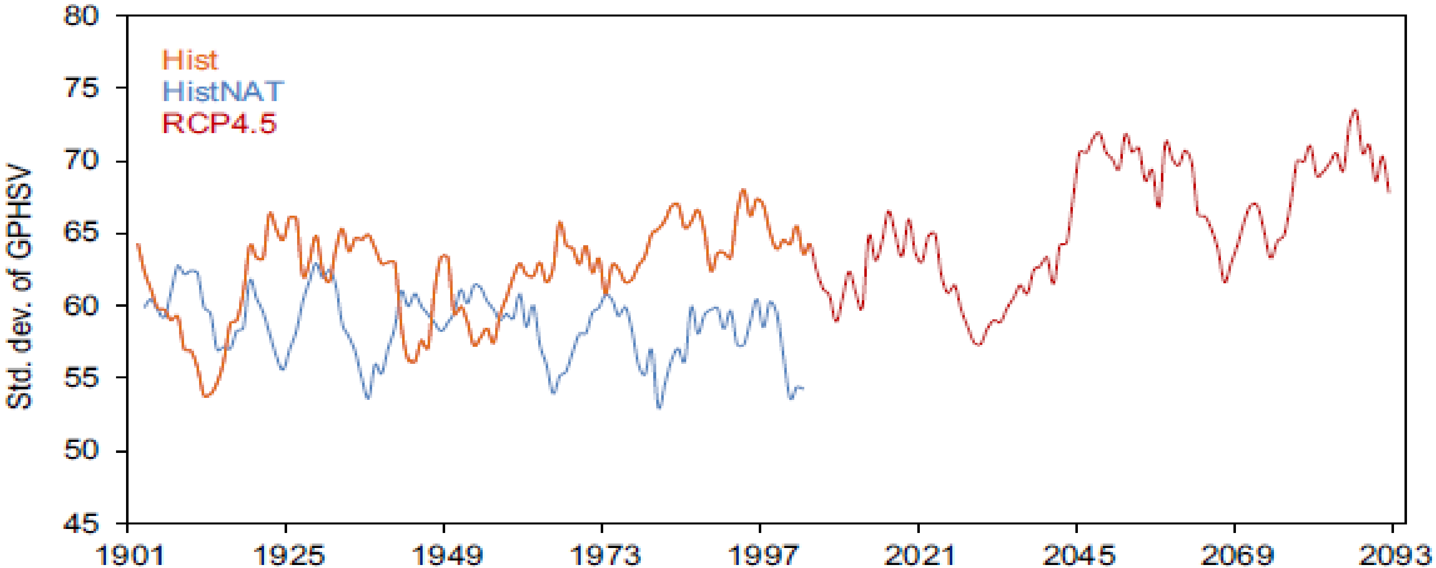

HIST, HISTNAT and RCP4.5

Krishnan et al. (2018)

Liu and Chen (2000)

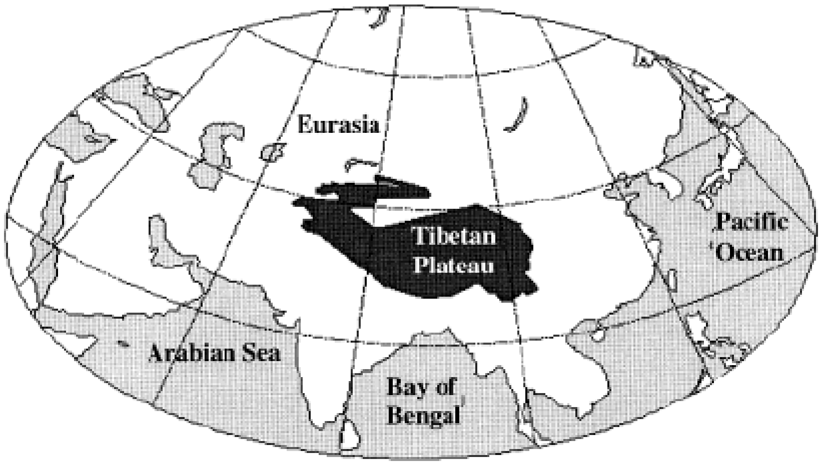

Map of the Tibetan Plateau (TP) domain. The black area approximately indicates the TP where the elevation is above 2000 m a.s.l

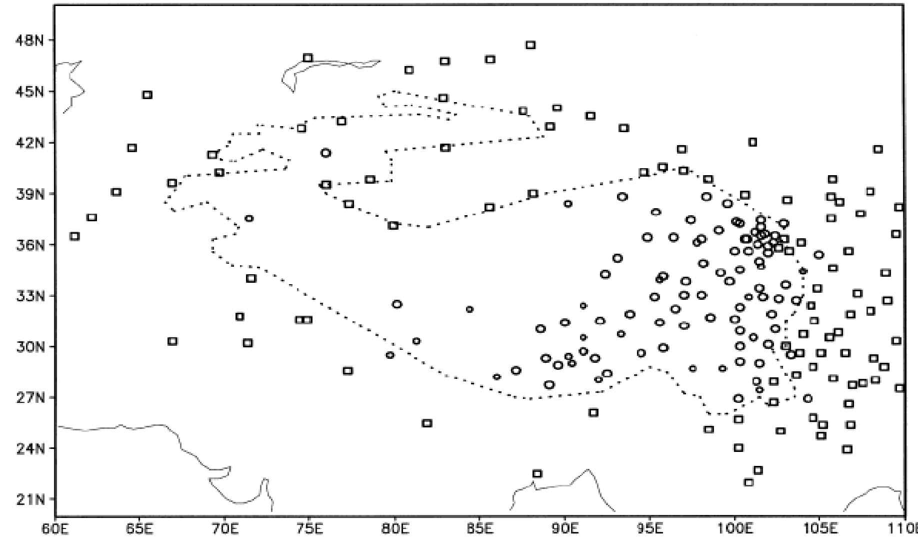

Location of the meteorological stations used. The circles and squares represent stations above and below 2000 m a.s.l respectively. The smaller circles show stations without continuous data during 1961-1990. The dotted line is the contour of the TP

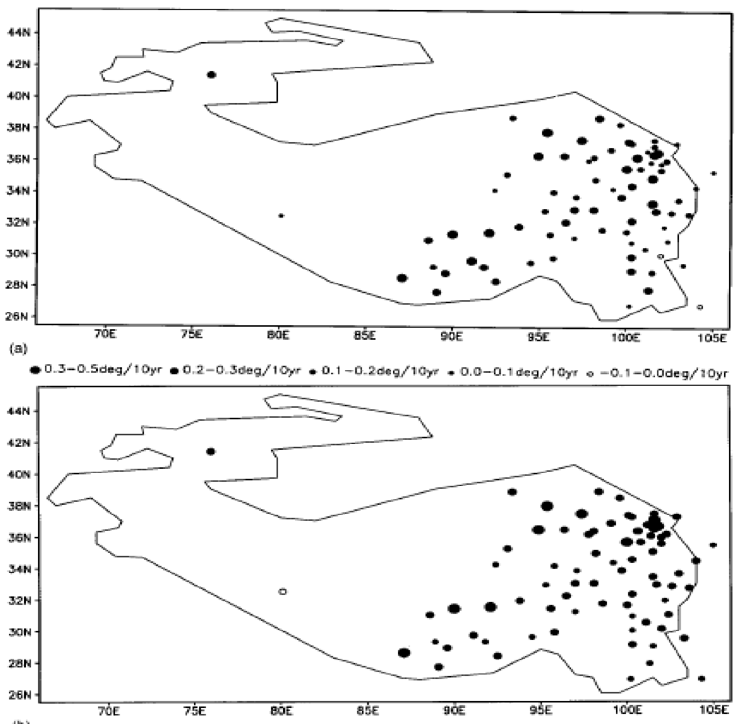

Surface temperature anomaly trends (1961 - 1990) in the TP (a) Annual (b) Winter

● 0.9–1.5deg/10yr ● 0.6–0.9deg/10yr ● 0.3–0.6deg/10yr ● 0.0–0.3deg/10yr ○ –0.3–0.0deg/10yr

Liu and Chen (2000)

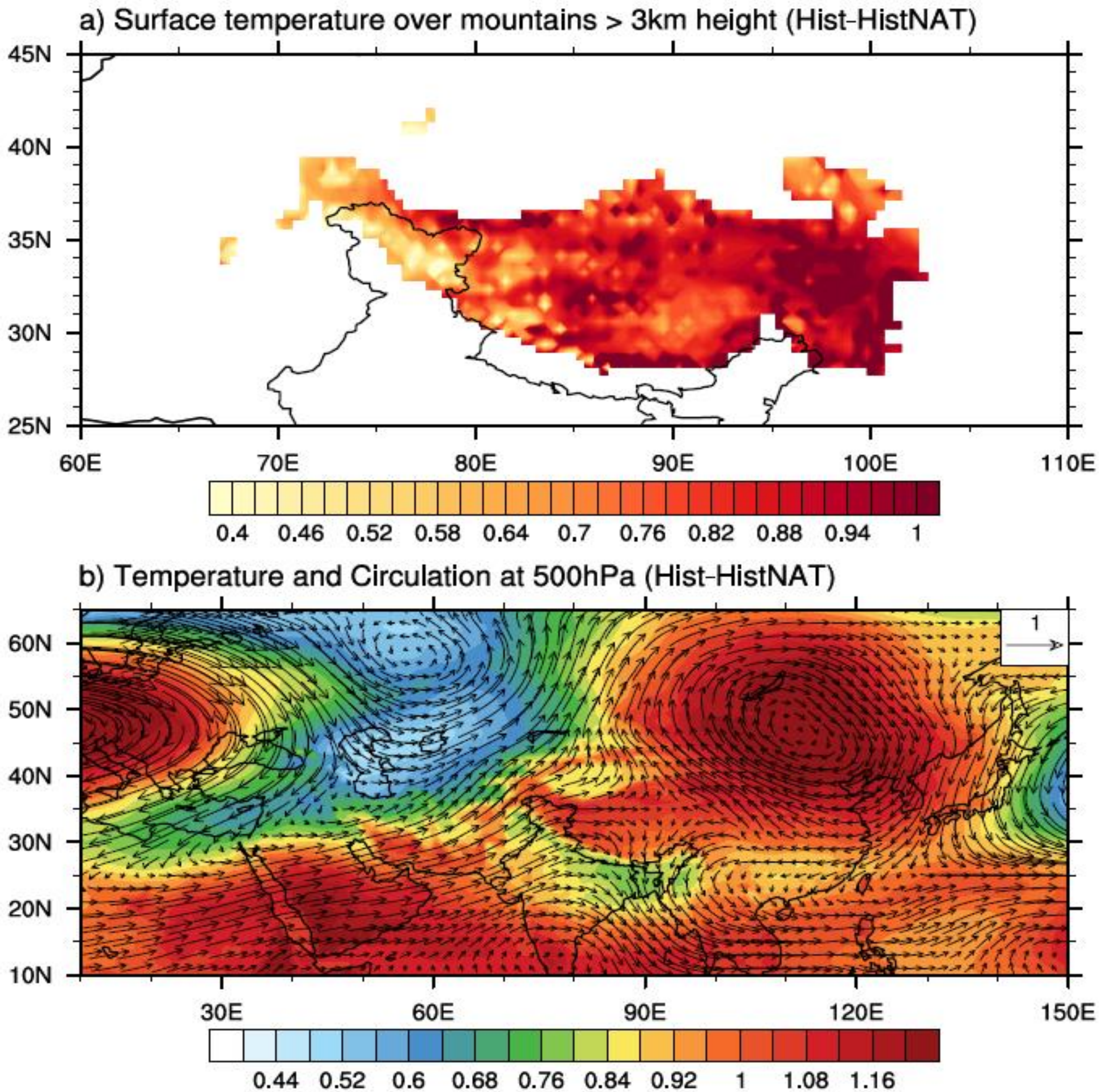

Krishnan et al. (2018)

Linear trends of different thickness layers from the HIST and HISTNAT simulations for the period 1951-2005. The units are m (55 yr)$^{-1}$. Red bars indicate trends calculated using the DJFMA layer thickness values averaged over the eastern Tibetan Plateau (90°E-120°E, 30°N-38°N) from the HIST experiment. Blue bars correspond to trends of thickness values averaged over the region to the west of the Tibetan Plateau (40°E-70°E, 30°N-38°N) from the HIST experiment. The corresponding trends from the HISTNAT experiment are shown by blue and red circles respectively.

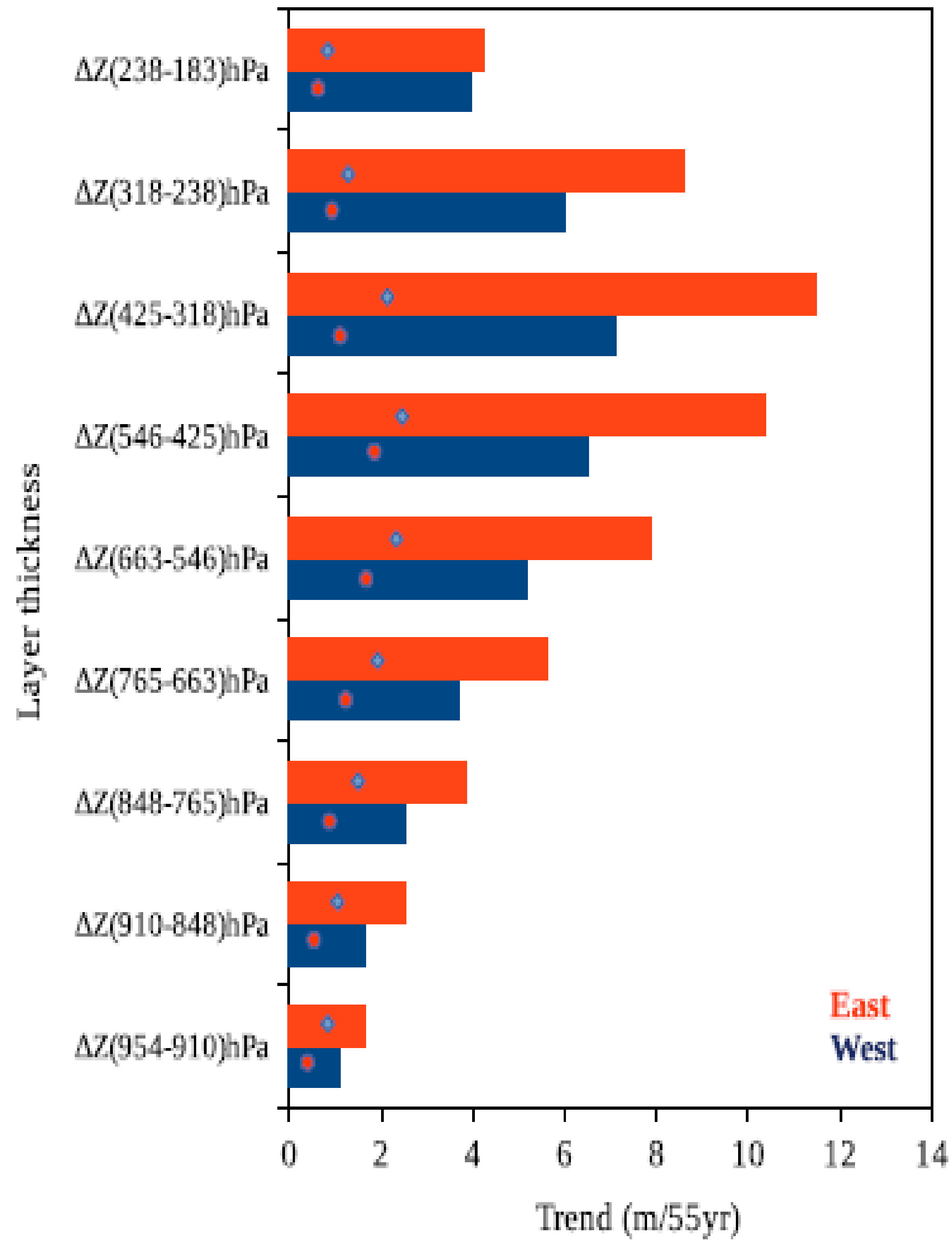

Summary

- Winter-to-early spring precipitation in the Western Himalayas (WH) primarily comes from eastward propagating weather systems from the Mediterranean region known as western disturbances (WDs). This is crucial for protecting the Karakoram-centered WH from significant snowmelt under warming climate.

- Increasing frequency of precipitation extremes in recent decades noted in some station observations located over the Western Himalayas

- Long-term climate change experiments were conducted at CCCR, IITM, Pune, using a global variable grid climate model with high-resolution zooming (grid size < 35 km) over South Asia

- Increasing trends in surface temperature and precipitation extremes over WH noted in the 20th century simulations and is attributable to human-induced climate change.

- Rising trend of simulated precipitation extremes over the WH region are found to concur with enhanced amplitude variations in the WD activity.

- Changes in background subtropical winds and mid-tropospheric temperature gradients associated with elevation dependency of the climate warming signal over the Tibetan Plateau.

- Simulations show snowfall enhancements in the high-elevation regions of the Karakoram and HKH due to enhanced amplitude variations of WDs. Declining tendency in snowfall amounts, associated with increased surface warming, is noted in the Central and Eastern Himalayas.

Thank you